American Mineralogist, Volume 101, pages 1543–1559, 2016

SPECIAL COLLECTION: PERSPECTIVES ON ORIGINS AND EVOLUTION OF CRUSTAL MAGMAS

Granitoid magmas preserved as melt inclusions in high-grade metamorphic rocks

Omar Bartoli[1,*], Antonio Acosta-Vigil[1,2], Silvio Ferrero[3,4], and Bernardo Cesare[1]

[1]Dipartimento di Geoscienze, Università di Padova, Via Gradenigo 6, 35131 Padova, Italy
[2]Instituto Andaluz de Ciencias de la Tierra, Consejo Superior de Investigaciones Científicas and Universidad de Granada, Armilla, Granada, Spain
[3]Institut für Geowissenschaften, Universität Potsdam, Karl-Liebknecht-Strasse 24/25, D-14476 Golm, Germany
[4]Museum für Naturkunde (MfN), Leibniz-Institut für Evolutions- und Biodiversitätsforschung, 10115 Berlin, Germany

Abstract

This review presents a compositional database of primary anatectic granitoid magmas, entirely based on melt inclusions (MI) in high-grade metamorphic rocks. Although MI are well known to igneous petrologists and have been extensively studied in intrusive and extrusive rocks, MI in crustal rocks that have undergone anatexis (migmatites and granulites) are a novel subject of research. They are generally trapped along the heating path by peritectic phases produced by incongruent melting reactions. Primary MI in high-grade metamorphic rocks are small, commonly 5–10 μm in diameter, and their most common mineral host is peritectic garnet. In most cases inclusions have crystallized into a cryptocrystalline aggregate and contain a granitoid phase assemblage (nanogranitoid inclusions) with quartz, K-feldspar, plagioclase, and one or two mica depending on the particular circumstances. After their experimental remelting under high-confining pressure, nanogranitoid MI can be analyzed combining several techniques (EMP, LA-ICP-MS, NanoSIMS, Raman). The trapped melt is granitic and metaluminous to peraluminous, and sometimes granodioritic, tonalitic, and trondhjemitic in composition, in agreement with the different P-T-a_{H_2O} conditions of melting and protolith composition, and overlap the composition of experimental glasses produced at similar conditions. Being trapped along the up-temperature trajectory—as opposed to classic MI in igneous rocks formed during down-temperature magma crystallization—fundamental information provided by nanogranitoid MI is the pristine composition of the natural primary anatectic melt for the specific rock under investigation. So far ~600 nanogranitoid MI, coming from several occurrences from different geologic and geodynamic settings and ages, have been characterized. Although the compiled MI database should be expanded to other potential sources of crustal magmas, MI data collected so far can be already used as natural "starting-point" compositions to track the processes involved in formation and evolution of granitoid magmas.

Keywords: Granitoid magmas, melt inclusions, nanogranite, crustal anatexis, peritectic phase

Introduction

Granitoid rocks and their extrusive counterparts represent the largest products of magmatic activity on continental crust. In zones of crustal thickening associated with collisional orogens, there are several examples of crystalline basements, which have experienced repeated episodes of high-temperature metamorphism, partial melting, and extraction of granitoid melts (Sawyer et al. 2011; Brown 2013). On the other hand, in continental margin arc systems there is much field and geochemical evidence of melting of crustal rocks and hybridization between crustal- and mantle-derived magmas, resulting in the formation of batholiths (Barnes et al. 2002; Annen et al. 2006; Kemp et al. 2007; Gray and Kemp 2009). Therefore, anatexis of crustal protoliths and formation of anatectic granitoid magmas are key processes for the formation of new crust and its geochemical differentiation (Brown and Rushmer 2006; Hacker et al. 2011; Sawyer et al. 2011). Field geology, experimental petrology, thermodynamic calculations, numerical modeling, whole-rock geochemistry and Hf-O isotopes in zircon represent the major tools for understanding the origin and evolution of anatectic granitoid magmas (see Annen et al. 2006; Brown 2013; Clemens 2006; Kemp et al. 2007; Sawyer et al. 2011; White et al. 2011). Despite the vigorous debate on the petrogenesis of granitoid magmas that began more than 60 years ago (Read 1948) conflicting views still exist, in particular concerning the melting processes at the source and the differentiation processes that modify granitoid chemistry (Clemens and Watkins 2001; Clemens and Stevens 2012, 2015; Brown 2013; Weinberg and Hasalovà 2015a, 2015b and discussion therein).

Here we present a novel and alternative method to investigate crustal magmas, providing a review of the current research on melt inclusions (MI) in high-grade metamorphic rocks, the source where crustal magmas originate. After discussing the origin of MI by incongruent melting in migmatites, granulites, and anatectic enclaves and presenting the data collected mainly by the research group of the authors, along with the adopted experimental and analytical strategies, we highlight how such tiny inclusions of melt can constrain the origin and evolution of granitoid magmas produced by anatexis of crustal rocks.

* E-mail: omar.bartoli@unipd.it
Special collection information can be found at http://www.minsocam.org/MSA/AmMin/special-collections.html.

Changing the viewpoint: Entrapment of melt inclusions upon heating

MI are small volumes of silicate melt enclosed in minerals (Roedder 1984). First recognized in the 19th century by Sorby (1858), MI hosted in minerals of igneous rocks have been long studied and widely used in the last 40 years (see data set reported in Kesler et al. 2013), becoming a worldwide-accepted technique to investigate melt evolution in magmatic systems (Clocchiatti 1975; Roedder 1979; Sobolev 1996; Frezzotti 2001; Schiano 2003; Bodnar and Student 2006; Thomas and Davidson 2012; Audétat and Lowenstern 2014; and references therein). These MI (hereafter "classic MI") are generally trapped during crystallization of magmas, i.e., along the cooling path where the host crystal is crystallizing from the melt that is being entrapped (Fig. 1). MI-bearing phenocrysts in lavas are a typical example of this mode of occurrence. Being trapped along the down-temperature trajectory (Fig. 1), such classic MI represent therefore snapshots on the liquid line of descent of silicate liquids (i.e., they represent variably evolved melts) and, particularly in the case of felsic systems, they have represented a key tool to investigate and understand the genesis of various ore deposits (Audétat and Lowenstern 2014 and references therein). Even in the case of entrapment by the first liquidus phase (for example olivine in some mantle-derived magmas), classic MI often approximate the composition of the parental melt (i.e., the most primitive melt found in an area) and not that of the primary one [i.e., the melt derived directly by partial melting of the source; see Fig. 1 in Bartoli et al. (2014)].

To represent primary melt compositions, MI should be entrapped in the source region, before magmas undergo segregation and differentiation processes such as mixing and/or mingling with other magma batches, double-diffusive convection, Soret diffusion, cumulus phenomena, fractional crystallization, volatile exsolution and assimilation of residual or exotic material (e.g., Burnham 1967; DePaolo 1981; Lesher et al. 1982; Barbarin 1988; Candela 1997; Weinberg et al. 2001; Stevens et al. 2007; Brown 2013). Indeed, all these processes produce final products—i.e., most of the extrusive and intrusive rocks we collect in the field—which are markedly different from the original melt produced at the source.

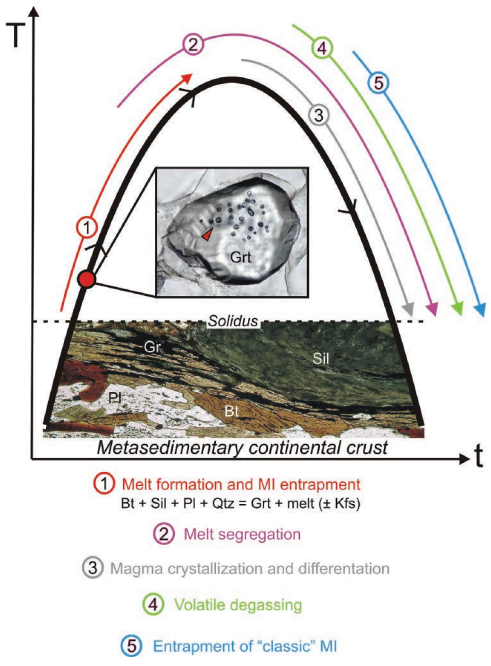

Figure 1. Schematic *T*-*t* diagram showing the main processes occurring during melt production (heating or prograde path) and melt consumption (cooling or retrograde path) in the partially melted continental crust. MI can be trapped during incongruent melting (arrow 1) and igneous crystallization (arrow 5). Mineral abbreviations after Kretz (1983). Ideal incongruent melting reaction from Vielzeuf and Holloway (1988).

The continental crust (i.e., the source region of the anatectic crustal magmas) mostly melts through incongruent melting reactions (Weinberg and Hasalovà 2015a and references therein). Along with magma crystallization, such reactions fulfill the fundamental requirement to form MI, i.e., the growth of a mineral in the presence of a melt phase. Indeed during incongruent melting, both a silicate liquid and a solid phase—the peritectic mineral—are produced contemporaneously along the up-temperature path (Fig. 1). In such a scenario, the peritectic phase can trap droplets of the melt with which it is growing. Shielded by the peritectic host, these MI can provide us with the pristine geochemical signatures ("the starting point" as stated by Sawyer et al. 2011) of magmas formed by crustal anatexis. Although the possibility of trapping droplets of melt during incongruent melting may appear intuitive, MI in high-grade metamorphic rocks have received only little consideration in the past decades. After the first detailed microstructural and microchemical description of MI in regionally metamorphosed granulites of southern India (Cesare et al. 2009), many other occurrences have been reported worldwide in the last six years (e.g., Cesare et al. 2011, 2015; Ferrero et al. 2012, 2014, 2015; Groppo et al. 2012; Mosca et al. 2012; Bartoli et al. 2013a, 2014; Darling 2103; Kawakami et al. 2013; Barich et al. 2014; Carosi et al. 2015; Massonne 2014), demonstrating that MI in high-grade metamorphic rocks are more common than expected. More rarely, MI have also been described in enclaves of partially melted continental crust brought to the Earth's surface in lavas. This is the case of the anatectic metasedimentary enclaves from the Neogene Volcanic Province (NVP) of southern Spain (Cesare et al. 1997—also known as "erupted migmatites," Zeck 1970). From all the above considerations it is clear that petrologists can utilize a novel tool, i.e., MI trapped by peritectic minerals, to gain previously unavailable information and to better understand the origins and evolution of crustal magmas.

Microstructural characterization of melt inclusions

In most migmatites, granulites, and anatectic enclaves investigated so far, MI have been mostly found in garnets of the melt-depleted melanosome portions of the rock (Table 1), because this mineral is the most common peritectic phase associated with crustal melting reactions in a wide *P*–*T*–*X* range (see Cesare et al. 2011; Ferrero et al. 2012 and references therein). Other MI-bearing phases are plagioclase and zircon, and less commonly cordierite, andalusite, ilmenite, hercynite, and monazite (Table 1; Cesare et al. 2015). Crustal enclaves contain abundant MI both in reactants and peritectic phases, e.g., plagioclase and garnet (Cesare and Maineri 1999; Cesare et al. 2003; Acosta-Vigil et al. 2007, 2010). Indeed,

TABLE 1. Occurrences of nanogranitoid melt inclusions discussed in the text

Locality	Host rocks	Host minerals	*T-P* conditions	Reference
Neogene Volcanic Province (NVP), SE Spain	Metapelitic enclave	Grt, Pl, And, Crd, Ilm	~615–850 °C, ~2–7 kbar	1, 2, 3, 4, 5, 6
Ojén, Ronda, S Spain	Quartzo-feldspathic metatexite	Grt	~660–700 °C, ~4.5–5 kbar	7, 8
Ojén, Ronda, S Spain	Quartzo-feldspathic diatexite	Grt	~820 °C, ~6–6.5 kbar	9
La Galite, Tunisia	Tonalitic and garnetitic enclave	Grt	~770–820 °C, ~5 kbar	10
Barun, Nepal Himalaya	Gneiss	Grt	~800–860 °C, ~8 kbar	11
Kerala Khondalite Belt (KKB), S India	Khondalites	Grt	~900 °C, ~6–8 kbar	11, 12
Orlica-Śnieżnik Dome, Bohemian Massif	Felsic granulite	Grt	~875 °C, ~27 kbar	13

Notes: 1 = Acosta-Vigil et al. (2007); 2 = Acosta-Vigil et al. (2010); 3 = Acosta-Vigil et al. (2012); 4 = Cesare et al. (2003); 5 = Cesare et al. (2007); 6 = Ferrero et al. (2011); 7 = Bartoli et al. (2013a); 8 = Bartoli et al. (2013b); 9 = Bartoli et al. (2015); 10 = Ferrero et al. (2014); 11 = Ferrero et al. (2012); 12 Cesare et al. (2009); 13 = Ferrero et al. (2015).

during melting with some degree of reaction overstepping, some reactant phases in the rock matrix may recrystallize, equilibrate with the melt and trap MI (Cesare et al. 2015).

From a microstructural point of view, MI may occur isolated, distributed in zonal arrangements, or in clusters with random distribution within the host mineral (Fig. 2; Ferrero et al. 2012; Barich et al. 2014). These modes of occurrence unequivocally demonstrate the primary nature of MI (Roedder 1979). MI are generally small (<20 μm) and often show negative crystal shape (Figs. 3a–3d). Locally, larger MI have been described [up to 150–200 μm, Barich et al. (2014); Ferrero et al. (2015)]. Variable degrees of crystallization have been observed and MI range from glassy to fully crystallized (Figs. 2e and 3a–3e). The most common daughter minerals found within crystallized MI are quartz, alkali feldspar, plagioclase, biotite, and muscovite (Figs. 3a–3c). In MI from near ultrahigh-pressure conditions, metastable polymorphs of albite, K-feldspar, and quartz have also been identified (Fig. 3b; see also Ferrero et al. 2016). A large number of minerals trapped during inclusion formation has been found within MI, the most common being graphite, zircon, rutile, and kyanite. Owing to the very fine grain-size (often <1 μm) and the granitic phase assemblage observed in totally crystallized MI, they have been referred to as "nanogranites" (Cesare et al. 2009). Because recent microchemical investigations have demonstrated the existence of granodiorite, trondhjemite, and tonalite compositions (Carosi et al. 2015; this study), the totally crystallized polycrystalline MI will be referred, hereafter, to as "nanogranitoid inclusions." Nanogranitoids can display a diffuse micro- to nano-porosity, which contains liquid H_2O, as evidenced by micro-Raman mapping (Bartoli et al. 2013a). Nanogranitoids may also coexist with primary C-bearing fluid inclusions (Fig. 3f). As both inclusion types are primary, they indicate conditions of fluid-melt immiscibility, thus suggesting COH fluid-present anatexis (Cesare et al. 2007; Ferrero et al. 2011). Preserved glassy MI are abundant in anatectic enclaves owing to the fast cooling (quench) related to the magma uprise and extrusion (Fig. 3d). On the other hand, nanogranitoids and partially crystallized MI are typically found in slowly cooled, regionally metamorphosed migmatite and granulite terranes (Figs. 3a–3c). Surprisingly, some preserved glassy MI coexisting with nanogranitoids have been recognized also in migmatitic terranes (Fig. 3e; see also Cesare et al. 2009; Bartoli et al. 2013a, 2013b; Barich et al. 2014). This geological oddity (i.e., the glass preservation in slowly cooled rocks) has been ascribed to either pore size effect (Cesare et al. 2009), the heterogeneous distribution of nucleation sites (Ferrero et al. 2012), or the high viscosity of the trapped melt (Bartoli et al. 2015).

CHEMICAL CHARACTERIZATION OF MELT INCLUSIONS

Re-melting nanogranitoid inclusions

The experimental re-melting of nanogranitoid inclusions is a prerequisite to retrieve the original composition (in terms of major and volatile contents) of the trapped melt. Because anatexis takes place in rocks of the middle to lower continental crust, at the bottom of thickened continental crust, and even in continental materials subducted to mantle depths, re-melting experiments of nanogranitoids must be performed under high confining pressure, using a piston-cylinder apparatus, to prevent the inclusion from decrepitating, volatile loss, and melt contamination. Indeed, as a consequence of the H_2O loss, crystallized inclusions can be completely re-melted only at temperatures higher than the trapping—i.e., H_2O loss results in an increased solidus temperature—leading to an inevitable melt-host interaction (see details in Bartoli et al. 2013c). The first attempts to remelt nanogranites using the routine technique in igneous petrology, namely the high-temperature heating stage at ambient pressure (Esposito et al. 2012), produced the decrepitation of the nanogranitoid inclusions, making them poorly suited for a geochemical study (Cesare et al. 2009).

The *P-T* conditions to be used during piston-cylinder remelting should be initially established based on phase-equilibria modeling or classic thermobarometry, which can provide a fair estimate of the (presumed) *P-T* conditions of MI entrapment (Bartoli et al. 2013a, 2013c; Ferrero et al. 2015). Conditions of further experiments are then fine-tuned based on the results of the first runs. Despite the time consuming pre- and post-run sample preparation (compared to the heating stage method), and the trial-and-error nature of the experimental approach, this method can successfully re-melt the nanogranitoids under high-confining pressure (see Bartoli et al. 2013c; Ferrero et al. 2015).

Building up the compositional database

Working with MI in partially melted rocks (i.e., their identification, re-homogenization, and chemical characterization) is challenging due to their small diameter, often <20 μm (Figs. 2 and 3). Despite these difficulties, originally glassy and successfully re-melted MI can be analyzed for the concentrations of most elements in the periodic table. Major element contents are routinely measured by electron microprobe (EMP), analyzing secondary standards in the same analytical session to monitor the alkali migration process and eventually calculate correction factors (Ferrero et al. 2012). Indeed, the small size of MI often demands the use of a beam diameter of ~1 μm (Bartoli et al. 2013a), resulting inevitably in Na loss during EMP analysis of hydrous felsic glasses (Morgan and London 1996, 2005a). The laser ablation-inductively

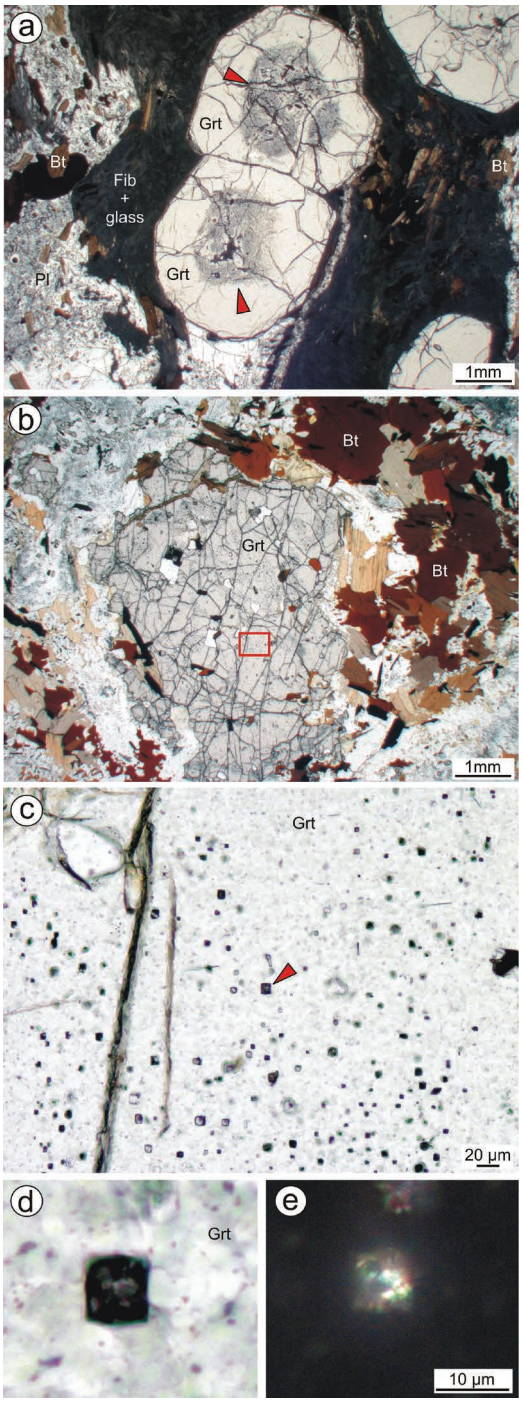

Figure 2. Photomicrographs of primary nanogranitoid inclusions. (**a**) Garnet porphyroblasts from a partially melted pelitic enclave from El Hoyazo, SE Spain (additional information in Cesare et al. 1997). MI are distributed in zonal arrangements (red arrows). (**b**) Peritectic garnet in porphyroblastic gneisses from the anatectic sequence of Jubrique, Betic Cordillera, S Spain (see also Barich et al. 2014). Square = area enlarged in **c**. (**c**) Close-up of inner part of the garnet crystal in **b** where clusters of micrometric inclusions are present. The presence of MI clusters with random distribution unequivocally demonstrates their primary nature. (**d** and **e**) Plane-polarized and crossed polars images, respectively of the crystallized inclusion marked by a red arrow in **c**. Multiple birefringent phases are recognizable within the inclusion.

coupled plasma-mass spectrometry (LA-ICP-MS) has been used to measure trace element contents of MI, drilling the glassy MI exposed on the host surface or the nanogranitoid inclusions entirely enclosed in the host. In the latter case, one of the major elements measured by EMP in coexisting glassy or re-melted MI can be used as internal standard for the deconvolution of the mixed signal (Halter et al. 2002). H_2O, which is the most important volatile dissolved in crustal magmas (Burnham 1975), can be quantified by different methods: deficiency from 100% in the EMP analysis (Acosta-Vigil et al. 2007), Raman spectroscopy (Bartoli et al. 2013a; Ferrero et al. 2015), and secondary ion mass spectrometry (SIMS/NanoSIMS: Bartoli et al. 2013c, 2014). Using NanoSIMS and Raman spectroscopy, the H_2O concentration of glass can be determined with a high spatial resolution of 1–2 µm. Bartoli et al. (2014) applied different methods to measure H_2O in MI from amphibolite-facies migmatites and observed that, compared to NanoSIMS concentrations, the difference of EMP totals from 100% generally yields slightly higher-H_2O contents (up to ~15% relative), whereas Raman spectroscopy underestimates H_2O (up to approximately 20% relative) when compared to NanoSIMS values. Ferrero et al. (2015) reported lower differences between H_2O values determined by Raman and EMP difference method (~9% relative on the average value).

By applying all these techniques, ~600 MI—including re-melted nanogranitoids in migmatites and granulites and glassy MI in anatectic enclaves—have been characterized to date (Fig. 4), leading to the construction of an extensive geochemical database of MI in high-grade metamorphic rocks. In detail, the compositional database consists of ~600 and ~200 major and trace elements analyses, respectively, and ~140 measurements of H_2O by either SIMS, NanoSIMS, or Raman. The interested reader may refer to the Supporting Information (Supplementary Tables[1] 1 and 2) and to Cesare et al. (2015) for tables where all the presented and discussed analyses are reported.

The analyzed MI come from three continents (Europe, Asia, and Africa) and are related to different geologic and geodynamic settings (Table 1) such as: (1) the late orogenic, low-to-medium *P* extensional setting represented by the Neogene Volcanic Province of southern Spain; (2) the low-*P* dynamothermal aureole of Ojén (Betic Cordillera, S Spain); (4) the low- and medium-*P* collision-related magmatism of the Maghrebian (La Galite, Tunisia) and Himalayan (Kali Gandaki, Nepal) mountain belts, respectively; (4) the low-to-medium *P* and ultrahigh-*T* regional metamorphism of the Kerala Kondalite Belt (India); and (5) the near ultrahigh-*P* metamorphism of the Bohemian Massif (Orlica-Śnieżnik Dome, central Europe). MI have been found in peraluminous metasedimentary rocks and metaluminous metaigneous rocks, and are inferred to have formed at conditions varying from 670 to 950 °C and 4 to 27 kbar, from Proterozoic to Quaternary/Pleistocene (Table 1). A complete list of published occurrences of MI in migmatites and granulites, along with a description of the host rock and conditions of melting, is reported in Cesare et al. (2015). For the sake of completeness, it should be noted that the research group of the writers has recently found MI also in Proterozoic and Archean rocks from the Americas,

[1]Deposit item AM-16-75541, Supplemental Tables. Deposit items are free to all readers and found on the MSA web site, via the specific issue's Table of Contents (go to http://www.minsocam.org/MSA/AmMin/TOC/).

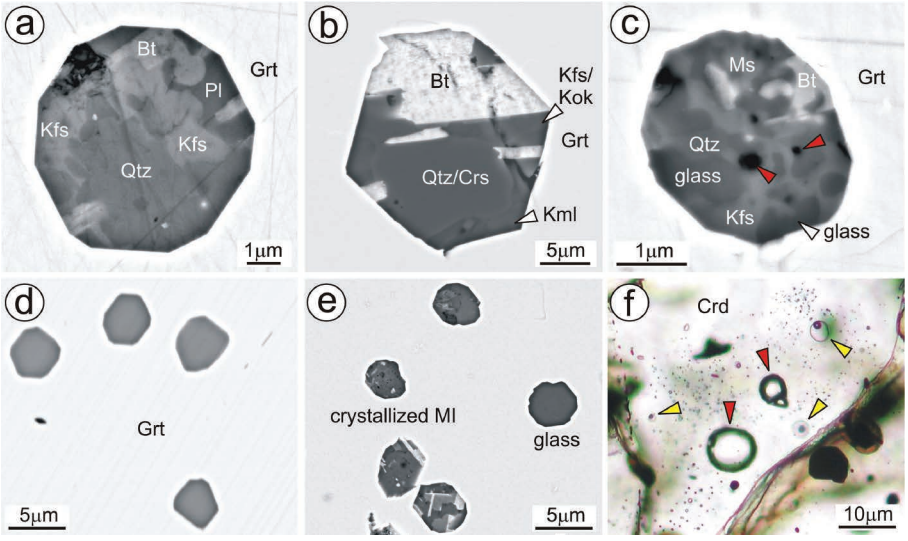

FIGURE 3. SEM backscattered images (**a–e**) and plane-polarized light photomicrograph (**f**) of the microstructures of melt inclusions. (**a**) Fully crystallized nanogranite in khondalites (India). (**b**) Fully crystallized MI from Bohemian Massif. In this case, polymorphs have been identified by Raman spectroscopy (Ferrero et al. 2016). (**c**) Partially crystallized inclusion with internal porosity (red arrows, respectively) from Ronda metatexites. (**d**) Glassy MI in anatectic enclaves from the Neogene Volcanic Province, SE Spain. (**e**) Coexistence of glassy and crystallized MI in Ronda diatexites. (**f**) Cluster of associated fluid and melt inclusions (red and yellow arrows), indicative of fluid immiscibility in a graphite-bearing crustal enclaves.

as well as, from Antarctica and Africa, but their microstructural and microchemical characterization is still in progress.

Reliability of the MI as records of melt compositions

During and after entrapment of melt its composition may be modified by several processes, making the MI unrepresentative of the bulk melt in the rock (Roedder 1984). Many processes such as the crystallization of the host on MI walls, the diffusional exchange of cations between the crystalline phases within nanogranitoids and the host mineral, the nucleation of bubbles by volume contraction and the retrograde fluid infiltration have been widely discussed by Acosta-Vigil et al. (2010, 2012), Bartoli et al. (2013c, 2014), and Cesare et al. (2015). Here, we consider two processes, with which igneous petrologists working with classic MI are more familiar: the boundary layer effect and diffusive H_2O re-equilibration.

Boundary layers may develop at the crystal-melt boundary, when the rate of crystal growth is faster than the rate of cation diffusion (Bacon 1989). This results in a layer immediately adjacent to the growing crystals that is generally depleted in compatible elements and enriched in incompatible elements (Kent 2008). If these boundary layer melts are trapped as MI, their chemical compositions are obviously not representative of the bulk melt. It should be noted, however, that: (1) examples of boundary layers have been mainly observed in experimental runs, whereas many studies on natural classic MI do not report compositions affected by boundary layer phenomena—see review papers of Kent (2008) and Audétat and Lowenstern (2014), and (2) experimental boundary layers commonly formed at high degrees of undercooling (~100–200 °C) around skeletal and dendritic crystals (e.g., Faure and Schiano 2005; Morgan and London 2005b). In particular, Faure and Schiano (2005) have demonstrated that the melt trapped in polyhedral crystals is representative of the parental melt, whereas the composition of MI hosted in skeletal or dendritic forsterite crystals lies away from the predicted liquid line of descent. It is important to stress again that MI in high-grade metamorphic rocks are trapped along the heating path in polyhedral peritectic crystals (as opposed to the MI formation during cooling/undercooling in crystallizing magmas). Results from a thorough study of primary MI hosted in garnets of migmatites from the Ojén unit (Betic Cordillera, S Spain) and formed at increasing temperatures (from ~700 to ~820 °C), show that MI compositions are mostly controlled by melting conditions, and not by boundary layer systematics. Thus, Fe (compatible with respect to the host garnet) and K (incompatible) are enriched in MI formed at higher temperatures, whereas low-temperature MI have higher H and Na (both incompatible) (Bartoli et al. 2014, 2015). Therefore, the boundary layer effect does not seem to have played an important role in shaping the geochemistry of these trapped melts. Likewise, mass balances show that boundary layer phenomena do not control the differences in major elements compositions among MI hosted in different minerals of anatectic enclaves of SE Spain (Cesare et al. 2015). Regarding the trace element concentrations, MI in several plagioclase and garnet crystals show remarkably similar concentrations in incompatible elements (e.g., Li, Rb, Cs, B, Be, Zn, As, Zr, Th, U), indicating that boundary layer phenomena are negligible for these elements. Conversely, the trace elements compatible or very slightly incompatible in the host (Sr, Ba, and Eu for plagioclase, and Y and HREE for garnet) are depleted in the MI due to interaction with the host phase (see Acosta-Vigil et al. 2012). In conclusion, the available data seem to indicate that MI are representative of the bulk melt for the major and incompatible trace elements.

Recently, the reliability of olivine-hosted classic MI in preserving the pre-eruptive H_2O contents of degassed lavas has been challenged by experimental studies, which have induced huge H_2O variations in MI within olivine (e.g., from ~3.8 wt% H_2O to ~800 ppm; Hauri 2002; Massare et al. 2002; Portnyagin et al. 2008; Gaetani et al. 2012). On the other hand, Audétat and Lowenstern (2014) have noted that most of the above experiments were done under unrealistic conditions and that many studies on natural MI in olivine demonstrate that the original volatile content of the trapped melt can be preserved after entrapment. Without entering in this "magmatic" dispute, we note that the two contrasting mechanisms of primary MI entrapment (i.e., on the liquidus during crystallization of magmas, and on or close to the solidus during incongruent melting of crustal rocks) along with the contrasting

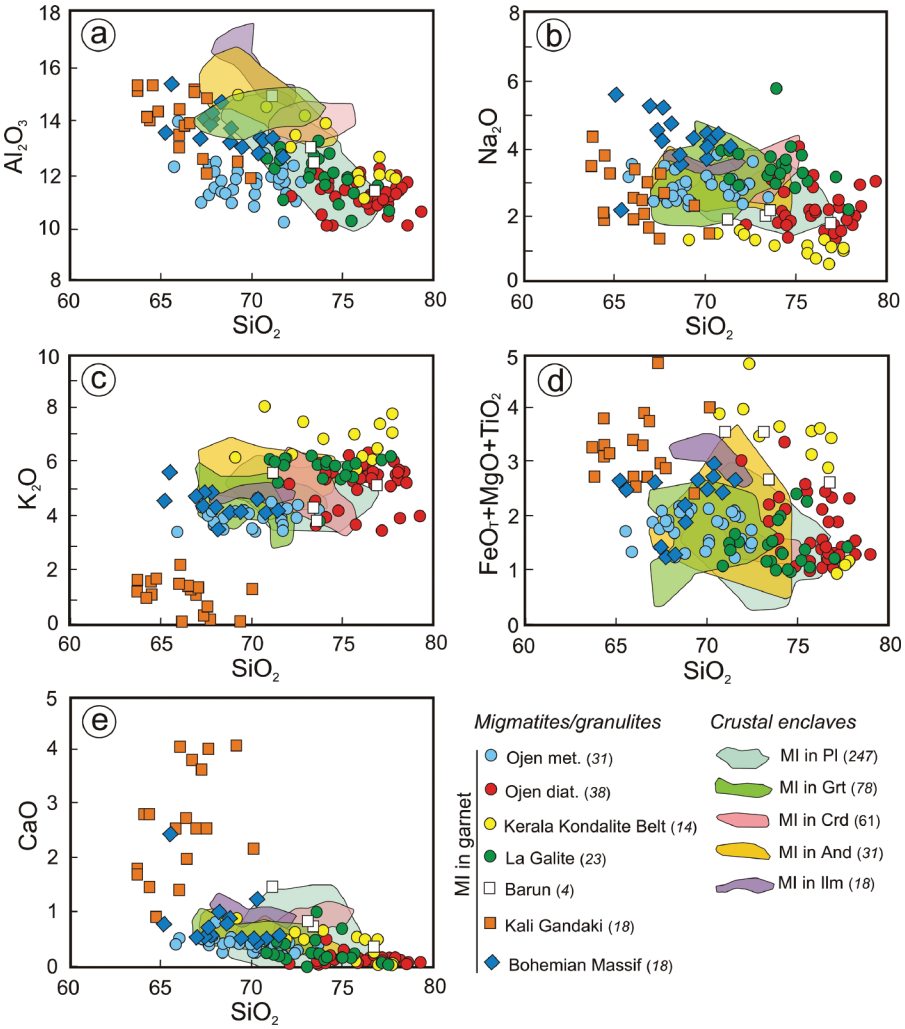

FIGURE 4. Harker diagrams showing the major element concentrations (wt%) of melt inclusions in crustal enclaves and in migmatites and granulites (data from Supplementary Tables 1[1] and 2[1]). (**a**) SiO_2 vs. Al_2O_3. (**b**) SiO_2 vs. Na_2O. (**c**) SiO_2 vs. K_2O. (**d**) SiO_2 vs. FeO_t+MgO+TiO_2. (**e**) SiO_2 vs. CaO. Numbers in parentheses indicate the number of analyses for each case study.

P-T histories may result in different processes affecting the H_2O content of the trapped melts. Compared with crystalline rocks, which have experienced prograde anatexis, olivine-hosted MI within magma batches represent the most suitable system for diffusive H_2O re-equilibration. Indeed, during ascent of magmas, important gradients of H_2O concentration and pressure can be continuously formed between the MI and the external magma. On the contrary, in the partially melted crust MI-bearing peritectic phases coexist with discrete fractions of melt scattered in a mostly solid matrix. As discussed by Bartoli et al. (2014), the large differences in physical parameters (e.g., temperature and, in turn, hydrogen diffusivities, pressure, and size of MI-bearing crystals) can result in times for the diffusive H_2O re-equilibration that are >10 orders of magnitude greater in migmatitic and granulitic terranes than in the plumbing of magmatic systems.

It might be argued that if crustal rocks undergo a long thermal history, reaching temperatures much higher than the trapping temperatures and producing higher amounts of melt, H_2O contents in MI could re-equilibrate with the external drier melt. In this case, three important observations must be taken into account. First, there is much field, microstructural, and geochemical evidence indicating that most of the crustal melts generated in the source area have been extracted (Brown 2013). Second, melt accumulation and extraction from anatectic rocks is expected to occur very early after crossing the solidus and to continue during the prograde path, at very low melt fractions (<0.07; Rosenberg and Handy 2005; Jamieson et al. 2011), leaving residual granulites enriched in peritectic minerals (Brown 2013). Third, very rapid rates of melt extraction have been reported in the literature. For example, Harris et al. (2000) and Villaros et al. (2009) calculated residence times of S-type granites at the source as short as 50 and 500 yr, respectively. Therefore, high-temperature conditions do not implicitly mean that MI in residual migmatites and granulites experienced diffusive H_2O re-equilibration. The successful re-homogenization of nanogranitoids at temperatures similar to those inferred by phase equilibria calculations or thermobarometry, as reported by Bartoli et al. (2013a, 2013c) and Ferrero et al. (2015), strongly supports the idea that MI can behave as a closed system. Rather, MI compositions could be compromised by fluid infiltration, hydration, and retrogression occurring during the subsolidus low-temperature evolution in crystalline basements. However, these processes leave clear microstructural evidence such as the presence of low-temperature minerals within the nanogranitoid inclusions like chlorite (replacing biotite) and pyrite [see Fig. 19 in

Cesare et al. (2015)]. All the above observations strongly suggest that the MI database corresponds to that of primary anatectic melts.

Major and trace elements, and H_2O contents

In general, the compiled compositional database for MI in high-grade metamorphic rocks reports compositions rich in SiO_2 (~64–79 wt%; on a hydrous basis), with variable Al_2O_3 (~10–18 wt%), Na_2O (~1–6 wt%), and K_2O contents (~0–8 wt%) (Fig. 4). Most MI have very low to low-moderate FeO_t+MgO+TiO_2 concentrations (~0.25–2.5 wt%), whereas a small fraction of the data set (~10%) show values up to ~4.0–5.0 wt%. CaO is low (<1.5 wt%), except for MI from Kali Gandaki where CaO content can reach values as high as 4 wt% (Fig. 4). H_2O shows extremely variable concentrations (0–12 wt%) that are related to different *P-T* conditions and fluid regimes during crustal melting.

Regarding the trace elements, to date the data set is limited to two case studies from S Spain, i.e., crustal enclaves from El Hoyazo and migmatites from Ojén. Despite the different tectonic settings, anatectic history, and host rocks and crystals, the trace elements patterns show remarkably similar characteristics when compared with the composition of the upper continental crust: MI are generally enriched in elements (Cs, Rb, Li, Be, and B) partially to totally controlled by muscovite and biotite, and depleted in elements (Ba, Th, REE, Sr, Zr, and Hf) hosted by feldspars and accessory phases (zircon and monazite) [Fig. 5; see also Fig. 13 of Acosta-Vigil et al. (2012)]. Overall, MI from Ojen migmatites are characterized by higher contents of Cs, Rb, B, U, Nb, Zr, Sm, V, and Zn, lower contents of Ba and Pb, and variable concentrations of Th, La, and Ce with respect to MI in NVP enclaves (Fig. 5). This may reflect differences in bulk host rock compositions and/or mechanisms of anatexis [i.e., different melting reactions, different extent of equilibration between melt and residuum; see Acosta-Vigil et al. (2010, 2012)].

One composition, different types of granitoids

Approximately 20 different classification schemes for granitoid rocks have been proposed in the last 40 yr (Barbarin 1999; Frost et al. 2001 and references therein). To describe the composition of crustal magmas trapped in peritectic phases of high-grade metamorphic rocks, we have followed some of the most commonly used classification schemes. Based on their normative compositions and considering the compositional fields of O'Connor (1965), the majority of MI analyzed up to date correspond to granites, whereas nanogranitoids from Kali Gandaki (Nepal) plot in the granodiorite, trondhjemite, and tonalite fields (Fig. 6). MI are generally slightly [ASI = 1.0–1.1; ASI = mol. $Al_2O_3/(CaO+Na_2O+K_2O)$] to strongly peraluminous, with ASI up to 1.5 (Fig. 7). However, some proportion of the MI enclosed in orthogneisses of the Bohemian Massif and tonalites of La Galite, are metaluminous or located at the boundary between the metaluminous and peralkaline fields (ASI = 0.8–1.0, alkalinity index up to –0.02) (Fig. 7). Chappell and White (1974) proposed the first, modern geochemical scheme for the classification of granitic (s.l.) rocks, and recognized two distinct granitoid types: the S-type (supracrustal type) derived from metasedimentary rocks and the I-type (infracrustal type) inferred to have formed from metaigneous sources (see also Chappell 1984, 1999; Chappell and White 1992, 2001). Considering their ASI, most analyzed MI corresponds to S-type granitoids, with only 8% of the MI plotting in the I-type field (Fig. 7). Remarkably, almost the totality of MI produced from anatexis of metaigneous rocks correspond to I-type granitoid compositions (Fig. 7).

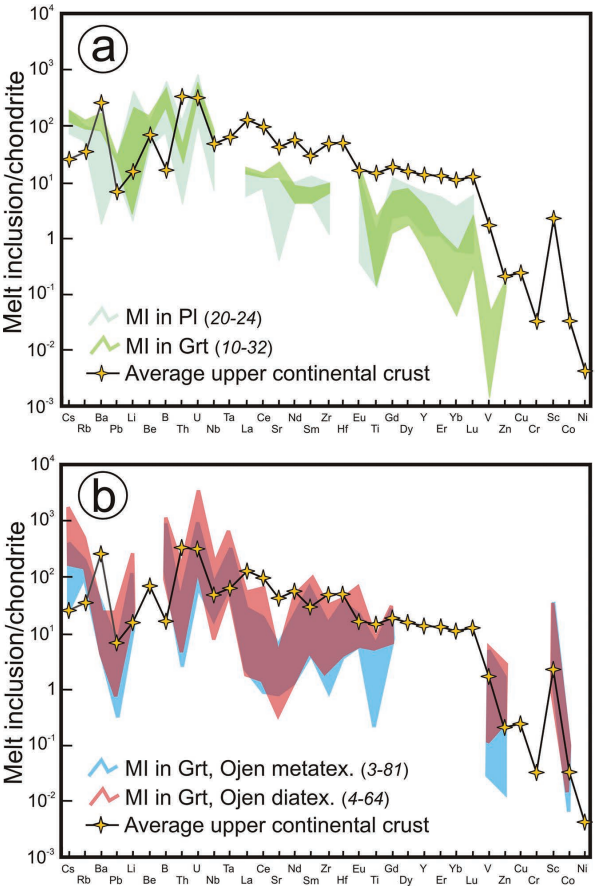

FIGURE 5. Chondrite-normalized trace element patterns (normalizing values from Sun and McDonough 1989). (**a**) Normalized trace element patterns for melt inclusions in crustal enclaves of NVP, SE Spain (from Acosta-Vigil et al. 2010). (**b**) Normalized trace element patterns for melt inclusions in migmatites from Ojen, S Spain (Bartoli, unpublished data). The average upper continental crust composition is reported for comparison (data from Rudnick and Gao 2014).

Frost et al. (2001) introduced a geochemical classification for granitoid rocks that has achieved wide use (see also Frost and Frost 2008). Using the compositional parameters suggested by these authors, MI are mostly ferroan granitoids, from alkali-calcic to calc-alkalic, even though some spread can be observed (Fig. 8). MI from Kali Gandaki rocks, instead, depart markedly from the other crustal melts and plot in the calcic field (Fig. 8). As stated by Frost and Frost (2008), calcic compositions are typical of melts produced by fluid-present melting.

INSIGHTS ON THE ORIGINS AND EVOLUTION OF GRANITOID MAGMAS

Melt inclusions and the model (haplo)granite system

The origin of granitoid rocks has been strongly debated in the middle half of the past century by N.L. Bowen and H.H. Read

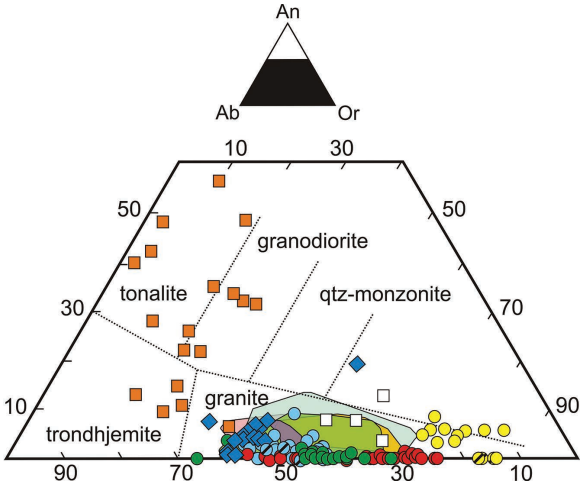

FIGURE 6. An-Or-Ab diagram with fields for granite, quartz-monzonite, granodiorite, trandhjemite, and tonalite after O'Connor (1965). Symbols as in Figure 4.

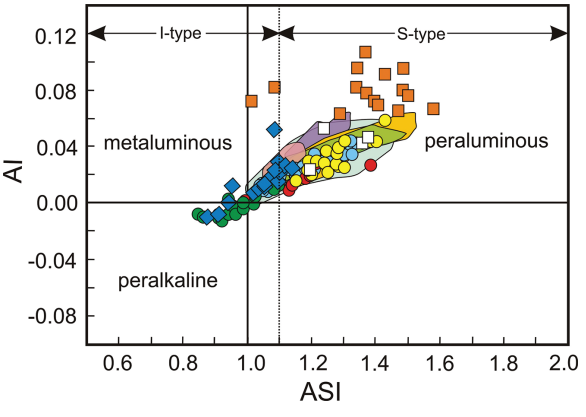

FIGURE 7. Plot of aluminum saturation index [ASI = molar Al_2O_3/($CaO+Na_2O+K_2O$)] vs. alkalinity index [AI = molar Al_2O_3-(Na_2O+K_2O); see Frost and Frost 2008]. Dotted line separates the compositional fields of I- and S-type granites s.l. (from Chappell and White 1974; Chappell 1999). Symbols as in Figure 4.

(see Bowen 1948; Gilluly 1948; Read 1948). This controversy ended a decade later, when the magmatic origin of granite (s.l.) was definitely demonstrated via experimental petrology by Tuttle and Bowen (1958). These authors showed that melting of a ternary mixture of quartz, albite, and orthoclase—i.e., a simple granitic system called haplogranite (Qtz-Ab-Or), starts at relatively low temperatures, typical of the continental crust, provided that the system is H_2O-saturated. After the pioneering work of Tuttle and Bowen (1958), an impressive number of studies have been performed to understand the effect of pressure and H_2O, and to a lesser extent of the other minor components, on the phase relations of the haplogranitic system (Johannes and Holtz 1996; see below). Also, whole-rock data have been often compared to the eutectic/cotectic compositions of haplogranite system to identify primary compositions of crustal melts (e.g., Olsen and Grant 1991; Symmes and Ferry 1995; Slagstad et al. 2005) or to infer the depth

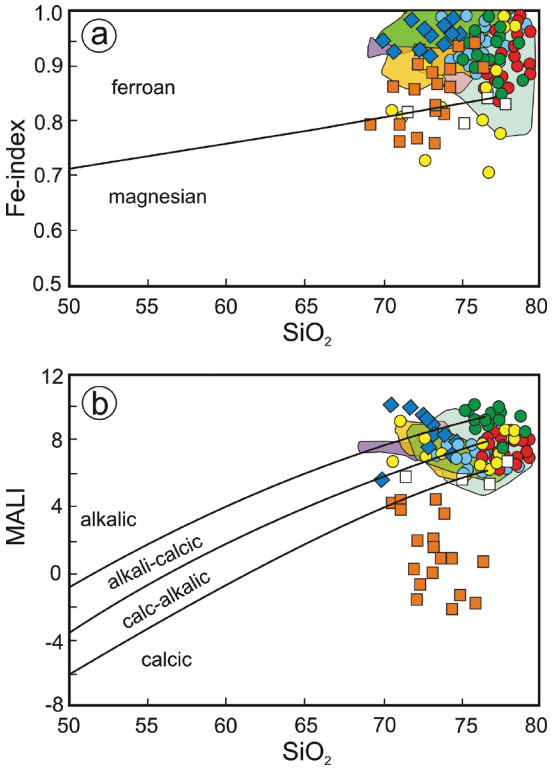

FIGURE 8. Geochemical classification of crustal melts following Frost et al. (2001) and Frost and Frost (2008). (**a**) Fe-index [FeO_T/(FeO_T+MgO)] vs. SiO_2 (wt%). (**b**) modified alkali-lime index (MALI = $Na_2O + K_2O$ – CaO) vs. SiO_2 (wt%). Data on a volatile-free basis. Symbols as in Figure 4.

of magma-storage (e.g., Blundy and Cashman 2001; Almeev et al. 2012; Gualda and Ghiorso 2013).

Because the haplogranitic system is a relevant reference frame to discuss granite petrogenesis, and because MI in high-grade metamorphic terranes seems to provide the compositions of the primary melts produced by melting of natural crustal rocks, it is important to see how MI data plot in the pseudoternary normative Qtz-Ab-Or diagram. Here, granitoid MI from each locality show some spread and a distinctive composition with respect to each other (Fig. 9a). They are commonly located toward the center of the diagram, often in the Qtz field and above the corresponding cotectic lines at the pressure of melting, between the H_2O-saturated eutectic point and the Qtz-Or join (Fig. 9a). Considering the relatively wide compositional spectrum of the host rocks, it is clear from Figure 9a that the concept of haplogranitic "minimum melt" composition finds little applicability in natural multi-component systems, as even low-temperature melts may significantly depart from eutectic compositions. Indeed, natural rocks are more complex than a model system such as the haplogranite, and additional components such as Ca, Ti, Fe, and Mg play an important role in modifying the liquidus and solidus phase relationships. For example, Wilke et al. (2015) noted that the effect of An on the phase relationships of the haplogranite system is much more pronounced if small amounts of Fe and Ti (~1 and ~0.2 wt%, respectively) are present.

In Figure 9b we have summarized the effects of *P*, H_2O, and other components (e.g., Al and Ca) on the position of the mini-

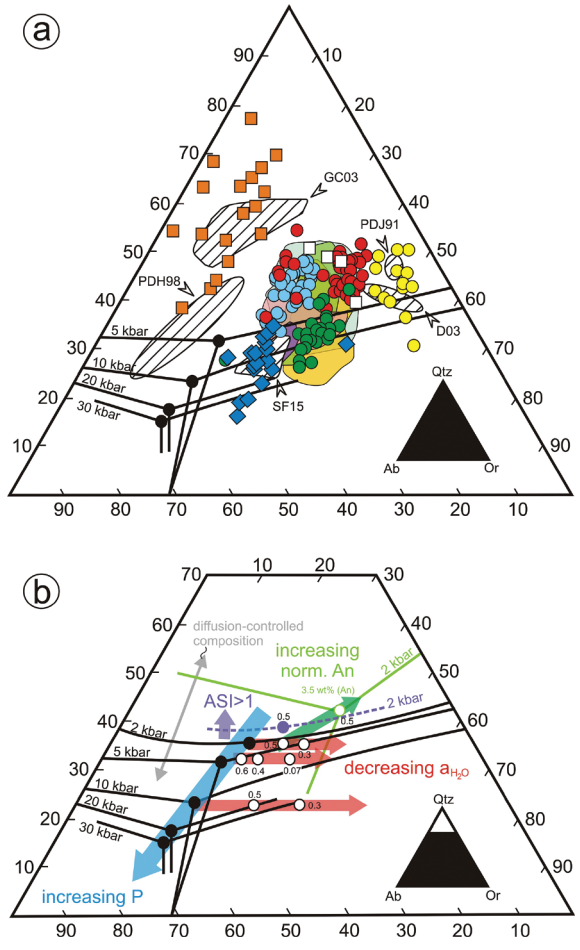

FIGURE 9. (**a**) CIPW Qtz-Ab-Or diagram showing the normative compositions of all analyzed nanogranitoid melt inclusions. Symbols as in Figure 4. Black dots and lines show the eutectic points and cotectic lines for the subaluminous haplogranite system at a_{H_2O} = 1 and different pressures (Holtz et al. 1992; Luth et al. 1964; Huang and Wyllie 1975). References to experimental glasses: PDJ91, 950 °C, 7 kbar (Patiño Douce and Johnston 1991); D03, 900 °C, 5 kbar (Droop et al. 2003); GC03, 675–775 °C, 6–14 kbar, H_2O-present (García-Casco et al. 2003); PDH98, 700–775 °C, 6–10 kbar, H_2O-present (Patiño Douce and Harris 1998); SF15: 870–950 °C, 16–30 kbar (see Ferrero et al. 2015). (**b**) Normative Qtz-Ab-Or diagram showing the displacement of eutectic points and cotectic lines as a function of *P*, a_{H_2O}, An, and Al_2O_3 contents. Black dots and lines as in **a**. Light blue arrow: effect of increasing pressure (Johannes and Holtz 1996 and references therein). Red arrows: effect of decreasing a_{H_2O} at 2, 5, and 10 kbar (white dots are eutectic points at different a_{H_2O}; Ebadi and Johannes 1991; Becker et al. 1998). Violet arrow: effect of increasing Al content at 2 kbar and a_{H_2O} = 0.5, i.e., from a subaluminous to peraluminous system (Holtz et al. 1992). Green arrow: effect of increasing An content at 2 kbar and a_{H_2O} = 0.5. With the addition of An the phase diagram changes to a eutectic system with respect to the haplogranite system with a minimum (see green lines; Wilke et al. 2015). Double gray arrow: effect of diffusive transport properties of the melt on the composition of experimental glasses (Acosta-Vigil et al. 2006). It should be noted that the addition of significant amounts of B and F to the system (>1 wt%) moves eutectic points and cotectic lines toward Ab-rich compositions (Johannes and Holtz 1996). However, the effects of B and F are not reported here because these elements are present in very low amounts in the investigated MI (<0.1 wt%; Acosta-Vigil et al. 2007). See text for details.

mum and eutectic points and of the cotectic lines in the ternary system Qtz-Ab-Or, as reported in the literature. MI often cluster above the corresponding cotectic lines, which, in accordance with experimental studies, suggests that excess Al and Ca play an important role in moving the eutectic compositions and the position of cotectic lines toward the Qtz apex (Figs. 9a and 9b). Most MI show some spread in the Qtz/feldspar ratio compared to their small variation in Ab/Or, forming trends at relatively high angle with the cotectic line (Fig. 9a). This spread of MI data parallel to the Qtz-feldspar direction suggests a control by diffusion in the melt for the major element compositions at the time of MI entrapment (Fig. 9b). Indeed, it has been experimentally shown that the sluggish diffusion of Si and Al vs. rapid diffusion of alkalis in granite melts produced by partial melting of quartzo-feldspathic protoliths result in linear trends in the Qtz-Ab-Or diagram [see Fig. 10 in Acosta-Vigil et al. (2006)].

The decrease of a_{H_2O} moves the eutectic point toward the Qtz-Or join without affecting the Qtz content (Fig. 9b). The majority of MI are located between the composition of the H_2O-saturated eutectic and the Qtz-Or side. Although this shift toward higher Or/Ab ratios can be partly related to the presence of Ca in natural systems (Fig. 9b), the collected data support the widespread idea that anatexis and formation of crustal melts generally occur under H_2O-undersaturated conditions (e.g., Thompson 1990; Clemens and Watkins 2001). It is important to note, however, that the absence or low proportion of H_2O-saturated melts does not represent a proof for fluid-absent melting, as even H_2O-fluxed melting is generally expected to produce final melts undersaturated in H_2O (Weinberg and Hasalovà 2015b).

The reduction of the a_{H_2O} during anatexis can be related to two different scenarios: (1) melting along a prograde path, in which all the free H_2O present in the rock below the H_2O-saturated solidus is dissolved in the melt at the solidus and melting then continues through fluid-absent reactions, and (2) presence of other components in excess fluids, like the carbonic species CO_2 and CH_4, that reduce the activity of H_2O. A clear example of scenario 1 is represented by the Ojén MI. The peraluminous metagraywacke of Ojén underwent prograde anatexis and MI in metatexites represent the first melt produced immediately beyond the fluid-saturated solidus at ~660–700 °C, ~4.5–5 kbar (Bartoli et al. 2013c), whereas MI in diatexites reflect the composition of melt formed at higher temperature, under H_2O-undersaturated conditions (~820 °C; Bartoli et al. 2015). In agreement with this evolution and with the bulk-rock composition, MI in diatexites show higher Or/Ab compared to MI in metatexites (Fig. 9a; see also Bartoli 2012), and the H_2O content of MI decreases from ~7 to ~3 wt% with increasing temperature (Bartoli et al. 2015).

In scenario 2, the presence in the fluid of carbonic species characterized by low solubility in granitoid melts can result in the phenomenon of immiscibility. As a matter of fact, cordierite, garnet, and plagioclase crystals from enclaves of the NVP (SE Spain) preserve spectacular microstructural evidence of immiscible trapping (Fig. 3f), where granitic MI coexist with primary fluid inclusions that are CO_2-dominated (>85 mol%), with minor amounts of N_2 and CH_4, and traces of CO and H_2 (see Cesare et al. 2007; Ferrero et al. 2011). Fluid-melt immiscibility is also documented in metaluminous granitoids at La Galite, Tunisia (Ferrero et al. 2014). The origin of CO_2-rich fluids in the deep

crust is strongly debated (Santosh and Omori 2008; Huizenga and Touret 2012). In the graphite-bearing enclaves from NVP the occurrence of CO_2 has been interpreted as internally generated by Fe^{3+} reduction and graphite oxidation during incongruent melting of biotite (Cesare et al. 2005). Conversely, infiltration of CO_2 from the mantle or from other crustal sources has been postulated for rocks from La Galite (Ferrero et al. 2014).

MI from Kerala Khondalite Belt (India) plot very far from haplogranitic minimum melts, close to the Qtz-Or sideline and point to melting temperatures well above minimum or eutectic temperatures, in agreement with the ultrahigh-temperature (>900 °C) origin of the rocks and the very low-H_2O content (~0.7 wt%; Cesare et al. 2009) of the MI. Similar compositions have been obtained by experimental melting of pelitic protoliths at 5–7 kbar, 900–950 °C (Fig. 9a). On the other hand, nanogranitoids from Kali Gandaki (Nepal) are clearly displaced toward the Qtz-Ab sideline and reflect the compositions of crustal melts produced by H_2O-fluxed melting (Carosi et al. 2015). The latter inclusions show the highest H_2O contents (up to 12 wt% by EMP differences) and CaO, and the lowest K_2O (Fig. 4), partly overlapping the composition of experimental glasses produced in the presence of excess H_2O at variable *P-T* conditions (6–14 kbar, 675–775 °C; Fig. 9a). Indeed, the presence of free H_2O decreases the plagioclase + quartz solidus more strongly than it depresses the stability of micas, producing tonalite/granodiorite/trondhjemite melts (Weinberg and Hasalovà 2015a and references therein). Melt inclusions from the orthogneiss of the Bohemian Massif, re-homogenized at 875 °C and 27 kbar, show the highest content of normative Ab (Fig. 9a) explained by melting at near ultrahigh-*P* conditions (increasing pressure moves haplogranitic eutectics closer the Ab apex; Fig. 9b). Experimental melts produced at 24–30 kbar, 870–950 °C by melting of different crustal protoliths plot in the same area (Fig. 9a; Ferrero et al. 2015).

Characterizing the melting processes at the source

Granitoid MI in high-grade metamorphic rocks are providing more and more robust and consistent information on the chemistry of natural crustal melts (see above). In addition, they represent a new tool to constrain mechanisms (i.e., melting reactions, melting mode, extent of equilibration with the solid residue) and conditions (*P-T-*a_{H_2O}) of formation of crustal magmas, and hence open a new window into the anatectic history of the partially melted continental crust (Fig. 1; Acosta-Vigil et al. 2010).

An example of this novel approach is the study of enclaves from El Hoyazo (Neogene Volcanic Province, SE Spain; Acosta-Vigil et al. 2007, 2010, 2012). These rocks represent fragments of continental crust that underwent partial melting and extraction of about 30–60 wt% of granitic melt (Cesare et al. 1997; Cesare 2008). Here, melt (undevitrified glass owing to rapid cooling of the host dacitic lava) has been chemically investigated both within plagioclase and garnet (see compilation of Fig. 5) and in the rock matrix where it often occurs along foliation planes (i.e., the equivalent of leucosomes in regional migmatites and granulites). Melt inclusions show the highest concentrations of Li, Cs, and B, whereas the matrix glass is characterized by higher contents of first row transition elements (FRTE), Y, Zr, Th, REE, and higher Rb/Cs and Rb/Li (Fig. 10a; see Acosta-Vigil et al. 2010). The concentrations of Zr and LREE were used to calculate the zircon and monazite saturation temperatures (Watson and Harrison 1984; Montel 1993), to link MI and potential melt-producing reactions. This approach represents an important advance in granitoid petrology, as the initial temperature of magmas at the source has been long considered to be an inaccessible parameter for allochthonous granites (see Miller et al. 2003). Melt inclusions in plagioclase yield the lowest temperatures (~665–715 °C), whereas MI in garnet (~685–750 °C) and matrix glass (~695–800 °C) show higher temperatures (Fig. 10b). Because the analyzed melts seem to be undersaturated to some extent in the accessory phases (Acosta-Vigil et al. 2012), the obtained temperatures have to be considered as minimum estimates (Miller et al. 2003; Acosta-Vigil et al. 2010). In summary, based on the composition of MI within several hosts and matrix glasses, calculated accessory mineral saturation temperatures, and microstructural relationships, it was concluded that the deep crust beneath the Neogene Volcanic Province of SE Spain underwent rapid heating and melting: MI in plagioclase reflect the earliest granitic melts produced by fluid-present to fluid-absent muscovite melting, whereas MI in garnet were produced simultaneously to slightly later via fluid-absent melting of muscovite (Fig. 10c). In contrast, the generation of granitic melts characterized by higher contents of FRTE and REE (the matrix melt) occurred at higher temperatures by biotite dehydration-melting reactions (Fig. 10c). In all cases melt and residual minerals were at, or close to, equilibrium with respect to most trace elements, except for garnet, and some undersaturation in accessory minerals (Acosta-Vigil et al. 2012).

The "starting-point" composition

To understand which granitoid rocks reflect primary crustal melts and, subsequently, what changes crustal magmas have undergone either near the source region or during their journey toward Earth's surface, "starting-point" compositions are required (Sawyer et al. 2011). Because leucosomes commonly do not represent primary melts (Sawyer 2008 and discussion therein), a widespread approach among crustal petrologists is to assume the composition of experimental glasses as representative of crustal melt composition at the source, and to use such composition in mass-balance calculations to track the processes involved in magma evolution and crustal differentiation (e.g., Milord et al. 2001; Solar and Brown 2001; Barnes et al. 2002; Guernina and Sawyer 2003; Stevens et al. 2007; Sawyer 2008; Hacker et al. 2011).

The fundamental advance provided by the study of nanogranitoid MI in high-grade metamorphic rocks is that they make accessible the composition of the natural primary anatectic melt for the specific rock under investigation at its specific *P-T-*X_{H_2O} conditions (Bartoli et al. 2013a; Ferrero et al. 2015; this work). Despite the number of MI analyses is already significant (see above), the compiled MI database should be expanded to cover other potential sources of crustal magmas (e.g., intermediate to mafic protoliths) and a wider spectrum of *P-T-*a_{H_2O} conditions under which continental crust may melt (i.e., to date the number of MI case studies is still quite low compared to the number of experimental studies). However, the already significant MI data set collected so far can be already useful to start discussing some of the previously proposed inferences and models regarding crustal melting and the formation and evolution of granitoid magmas. Clearly, to make inferences on petrogenetic processes affecting

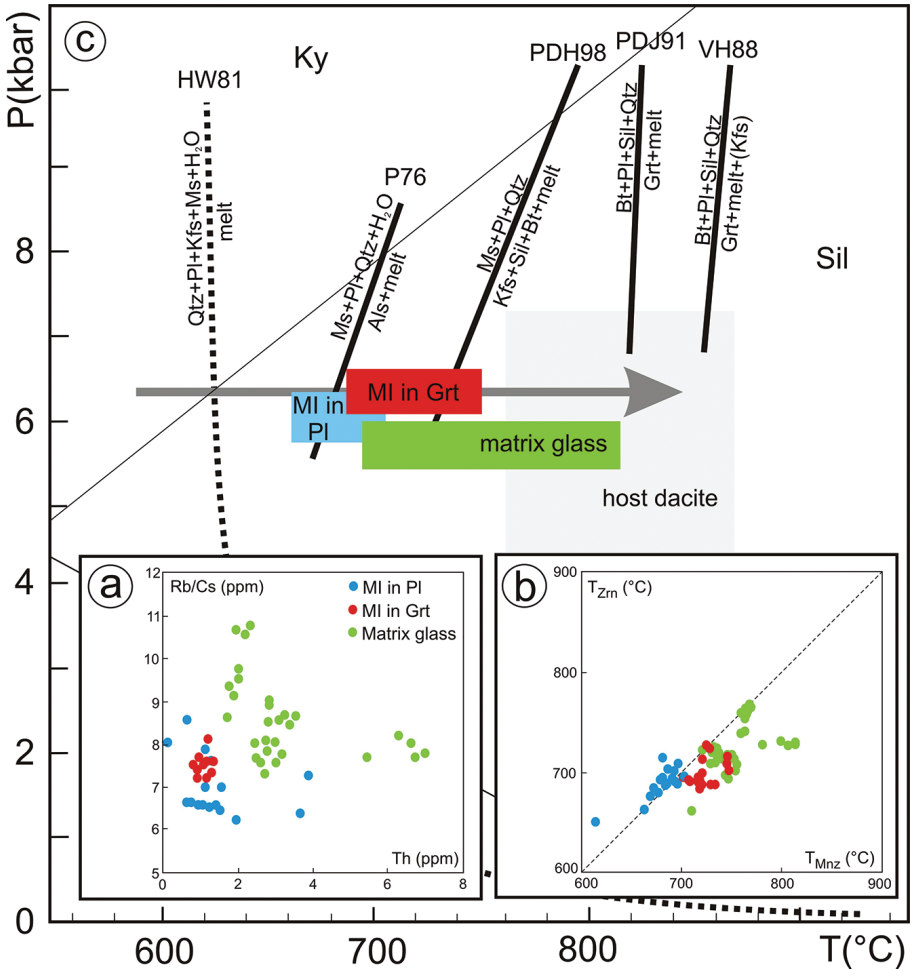

FIGURE 10. (**a**) Variation diagram showing the trace element contents for glassy MI and matrix glass in the crustal enclaves hosted in El Hoyazo dacite (NVP, SE Spain). (**b**) Zircon and monazite saturation temperatures calculated for all analyzed glasses of enclaves. Symbols as in **a**. Diagonal line marks the geometrical location of points where both temperatures coincide. (**c**) Prograde history of melt formation in the continental crust beneath the Neogene Volcanic Province of SE Spain, estimated by accessory mineral saturation temperatures (redrawn after Acosta-Vigil et al. 2010). The relevant experimentally determined melting reactions in the granitic and metapelitic systems are reported. HW81 refers to Huang and Wyllie (1981), P76 to Peto (1976), PDH98 to Patiño Douce and Harris (1998), PDJ91 to Patiño Douce and Johnston (1991), and VH88 to Vielzeuf and Holloway (1988).

anatectic magmas, and in the absence of specific primary melt compositions from MI for their particular study area, authors should consider using the MI compositions in the published data set for the conditions (*P*-*T*-X_{H_2O}-bulk rock composition) closest to the particular rocks that they are investigating.

Figures 11a–11d provides the compositional variations of MI in terms of mol% of Fe_{Tot}+Mg+Ti, Na+Ca, K, and Si+Al. The major crystalline phases are reported along with MI data. These types of diagrams have been previously used to model crustal reworking by anatexis (see Solar and Brown 2001; Barnes et al. 2002; Korhonen et al. 2010; Farina et al. 2015; Yakymchuk et al. 2015). Host rock compositions form different clusters according to their nature (for example, metapelites show the highest Fe_{Tot}+Mg+Ti values, whereas metagraywackes are enriched in Si and K); MI plot away from the Fe_{Tot}+Mg+Ti apex, into the bottom half of the diagrams at variable (Na+Ca)/K and (Na+Ca)/(Si+Al) ratios, providing a slightly variable though distinctive melt composition (Figs. 11a–11d). This is in agreement with the fact that the composition of the source and conditions of anatexis play a major control on melt chemistry.

The Himalayan Leucogranites (HL) are commonly considered to represent nearly pure melts produced by low-temperature (~700 °C) melting of metapelites and metagraywackes (Le Fort et al. 1987). As a matter of fact, most HL overlap with the low-temperature MI (i.e., those hosted in garnet from the Ronda metatexites and in garnet and plagioclase of NVP enclaves), supporting their primary nature (Figs. 12e and 12f). Some HL compositions, however, do not resemble MI compositions and plot in the proximity of the lower portion of the field occupied by most MI data (Figs. 11e and 11f). It is important to note that the difference in mafic components (Fe, Mg, and Ti) between HL and MI cannot be related to contamination of MI by the host phase during analysis, as MI hosted in Fe-, Mg-, and Ti-free hosts such as plagioclase show similar and sometimes higher Fe+Mg+Ti contents with respect to MI hosted in garnet (Figs. 11b and 11d). On one hand, the observed discrepancy can be related to an incomplete MI data set (i.e., incomplete sampling of MI in high-grade metamorphic rocks). On the other hand, it could indicate a non-primary nature of some HL. For instance, Scailet et al. (1990) stated that some geochemical features of Gangotri leucogranites (for which compositions sometimes depart from those of MI; Fig. 11e) can be explained by fractionation of the early crystallizing phases. Their compositions often depart from the compositions of primary HL in the opposite direction of the Bt and Ms fields (Figs. 11e and 11f). As a matter of fact, some Gangotri leucogranites have lower Co, V, and B contents than MI in Ronda metatexites and lower Li content than MI in garnet of NVP, in agreement with a mica fractionation process. It should be noted that petrographic and

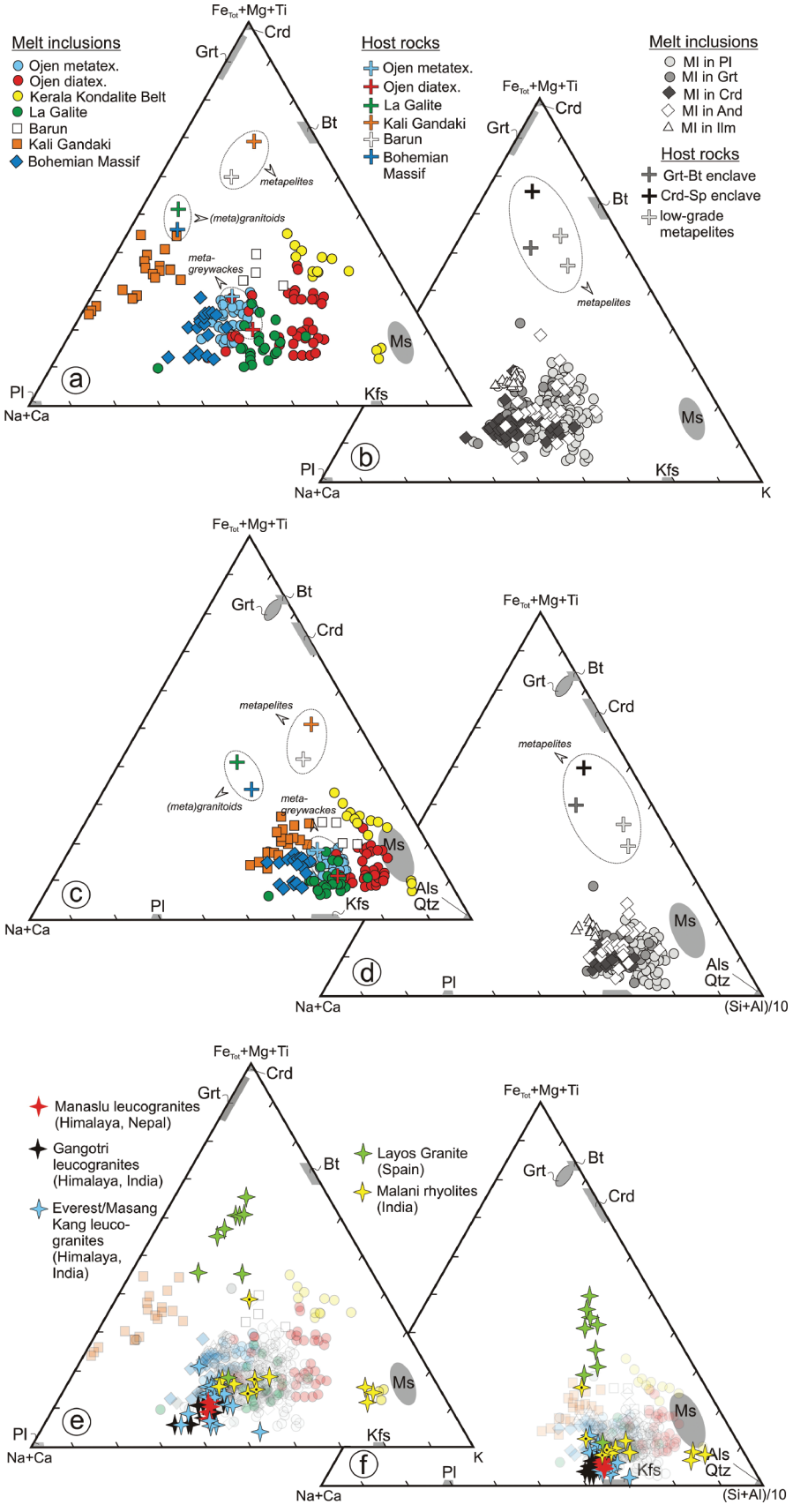

FIGURE 11. Compositions (in mol%) of analyzed nanogranitoid melt inclusions in terms of (Fe_{Tot}+Mg+Ti), (Na+Ca), (Si+Al)/10, and K (after Solar and Brown 2001; Barnes et al. 2002). The compositional fields of major crystalline phases and host rocks are reported. Bulk compositions of crystalline rocks are from Bartoli (2012), Groppo et al. (2012), Ferrero et al. (2014, 2015), and Iaccarino et al. (2015). Data for KKB rocks are not available. In the case of El Hoyazo samples, both chemical compositions of: (1) Grt-Bt and Crd-Sp enclaves, and (2) low-grade metapelites from the Alpujarride basement (considered to approximate the source composition before melt extraction) are plotted (data from Cesare et al. 1997). (**a** and **b**) (Fe_{Tot}+Mg+Ti)–(Na+Ca)–K diagrams for MI from crystalline rocks (**a**) and from crustal enclaves (**b**). (**c** and **d**) (Fe_{Tot}+Mg+Ti)–(Na+Ca)–(Si+Al)/10 diagrams for MI from crystalline rocks (**c**) and from crustal enclaves (**d**). (**e** and **f**) Comparison between MI and crustal magmas. Manaslu leucogranites: data from Le Fort et al. (1981, 1987) and Guillot and Le Fort (1995). Gangotri leucogranites: data from Scaillet et al. (1990). Everest/Masang Kang leucogranites: data from Visonà et al. (2012). Layos granite: data from Barbero and Villaseca (1992). Manali rhyolites: data from Maheshwari et al. (1996) and Sharma (2004). Yellow stars containing black dots indicate metaluminous or peralkaline Malani rhyolites. See text for details.

experimental evidence indicates that biotite was likely the first mineral to crystallize in many HL (Scaillet et al. 1995). Therefore, the available MI data seem to support a primary nature for the majority of HL, even though fractional crystallization processes might have occurred locally, in agreement with results from previous studies (i.e., Le Fort et al. 1987; Scaillet et al. 1990). It is important to note that MI from Kali Gandaki (Nepal) represent Ca-rich melts produced during Eocene prograde metamorphism (Carosi et al. 2015; Iaccarino et al. 2015) and, therefore, they are not related to the Miocene HL formed during exhumation stage (Harris and Massey 1994).

The Layos Granite (Toledo Complex, central Spain) represents a S-type, strongly peraluminous Crd-bearing granitoid suite, varying from quartz-rich tonalite to melamonzogranites and formed at about 800–850 °C by biotite melting of metapelites (Barbero and Villaseca 1992). Most of these rocks plot away from MI data sets, toward the Fe_{Tot}+Mg+Ti apex (Figs. 11e and 11f). The authors explained the observed compositional variability of the suite by a "restite unmixing" model (Barbero and Villaseca 1992). This model was proposed by Chappell et al. (1987) to explain the geochemical variability of granitoid rocks and states that the majority of granites represent mixtures between a low-*T* melt and the restite, i.e., solid materials that were residual from the source. Therefore, granites were thought to image their source in a simple way: compositional variations observed within granitoid suites reflect varying degrees of restite unmixing with a minimum or near-minimum temperature (haplogranitic) melt (Chappell et al. 1987). However, this model has received several criticisms from the geochemical, petrographic, and physical point of view (see Wall et al. 1987; Clemens and Mawer 1992; Clemens 2003; Vernon 2010; Clemens and Stevens 2012 for additional details). The fact that the composition of the primary melt produced in the source may differ markedly from that of minimum melt, as clearly demonstrated by MI study (see discussion above), demonstrates that the assumption that the melt component has an eutectic composition is not applicable in natural systems. Recently, Stevens et al. (2007) and Clemens and Stevens (2012) proposed a revised version of the restite unmixing model, called "peritectic assemblage entrainment" or "selective peritectic phase entrainment." Following this model, the more mafic granitoid rocks result from the entrainment of the solid peritectic products of the melting reaction to the melt (although how this would occur is not fully explained), rather than from the entrainment of a proportion of the total solid mineral assemblage remaining after the melting reaction. Regarding the Layos Granite, only one data point plots in the MI field (overlapping the composition of MI trapped in Crd from metapelites and formed at ~850 °C; Figs. 11e and 11f) and, in turn, seems to reflect a primary origin. The rest of data plots between this primary melt composition and the Fe_{Tot}+Mg+Ti apex and does not form a trend toward the (Si+Al)/10 apex. Similarly, in the (Fe_{Tot}+Mg+Ti)–(Si)–(Al) diagram (not shown), Layos granites do not show compositional trends toward the Si and Al apexes. According to the model proposed by Stevens et al. (2007), this chemical signature can be explained by differential entrainment of peritectic cordierite (up to 30% of Crd has been documented

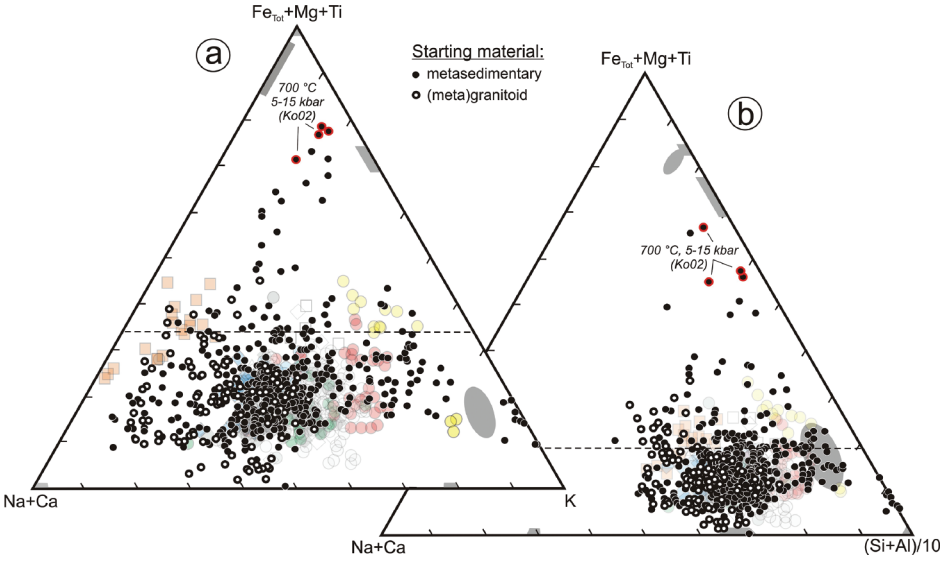

FIGURE 12. Comparison among the Fe_{Tot}+Mg+Ti, (Na+Ca), (Si+Al)/10, and K concentrations (in mol%) of melt inclusions and glasses from partial melting experiments. Experimental glasses were produced at T = 650–950 °C, P = 1–50 kbar, variable a_{H_2O} and from metasedimentary and felsic (SiO_2 ≥ 62 wt%) (meta)granitoid protoliths. Data from: Conrad et al. (1988); Le Breton and Thompson (1988); Vielzeuf and Holloway (1988); Brearley and Rubie (1990); Patiño Douce and Johnston (1991); Holtz and Johannes (1991); Skjerlie and Johnston (1993); Icenhower and London (1995 1996); Gardien et al. (1995, 2000); Patiño Douce and Beard (1995, 1996); Singh and Johannes (1996); Montel and Vielzeuf (1997); Patiño Douce and Harris (1998); Pickering and Johnston (1998); Castro et al. (1999); Litvinovsky et al. (2000); Koester et al. (2002); Nair and Chacko (2002); García-Casco et al. (2003); Droop et al. (2003); Grant (2004 2009); Schmidt et al. (2004); Spicer et al. (2004); López et al. (2005); Tropper et al. (2005); Acosta-Vigil et al. (2006); Auzanneau et al. (2006); Watkins et al. (2007); Hermann and Spandler (2008); Ward et al. (2008); Ferri et al. (2009). Compositions of melt inclusions and major crystalline phases as in Figure 11. Red dots: experimental glasses produced at 700 °C and 5–15 kbar (from Koester et al. 2002). Dashed black lines reflect the maximum Fe_{Tot}+Mg+Ti contents reported for low-temperature (650–720 °C) experimental glasses, with the exception of analyses reported in Koester et al. (2002). See text for details.

in these rocks), without the involvement of residual Qtz and Als, i.e., the restite unmixing model does not seem to be applicable in this specific case.

The Malani rhyolites (western India) are considered to be the product of high-*T* crustal anatexis (Maheshwari et al. 1996), and the fact that the majority of lava compositions match those of MI supports their primary origin (Fig. 11c). Strongly peraluminous, K-rich Malani rhyolites resemble the glassy MI from Kherala Khondalite Belt, in agreement with the inference that the rhyolites were likely produced by melting of metapelites at temperatures ≥850 °C (Maheshwari et al. 1996). At the same time, the comparison with MI would suggest a more complex scenario for the genesis of these anatectic lavas. Malani rhyolites have variable (Na+Ca)/K ratio and some lava compositions overlap the compositions of MI found in NVP metapelitic enclaves, Ronda metatexites and La Galite granodiorite and formed at variable temperatures (~700–820 °C) (Fig. 11c). These lavas range from peraluminous, through metaluminous to peralkaline. Notably, almost the totality of metaluminous/peralkaline lavas approach the metaluminous/peralkaline compositions of MI from La Galite granodiorite. The observed compositional variability can reflect the presence of distinct magma batches in the Malani rhyolite complex, formed and extracted during prograde heating of a compositionally heterogeneous crustal source. In this sense, other work has verified the occurrence of a heterogeneous crystalline basement (composed of both granodiorites, orthogneisses, and metasedimentary rocks) beneath Malani rhyolites (Pandit et al. 1999; Sharma 2004). Instead a single composition seems to reflect the entrainment of mafic minerals (Fig. 11c).

In Figure 12 we have compared the composition of MI with a data set of ~520 experimental glasses reported in literature and produced at variable *P-T-*a_{H_2O} conditions and using different starting materials, i.e., metasedimentary and felsic (meta)granitoid protoliths. Remarkably, MI and glasses from experiments seem to be characterized by similar compositions and compositional ranges, even though experimental melts may show higher Fe_{Tot}+Mg+Ti values than MI (Fig. 12). Koester et al. (2002) reported glasses, produced at 700 °C and 5–15 kbar, characterized by anomalously high FeO, TiO_2, and MgO contents (e.g., FeO ~9.5 wt%; see red dots in Fig. 12), in contrast with their low-temperature origin. The authors argued that the lack of chemical equilibrium was responsible for the heterogeneous chemical compositions of melt observed in near-solidus experiments (Koester et al. 2002; see also Gardien et al. 1995). Indeed, as any other petrologic tool, partial melting experiments may suffer from potential pitfalls, in particular: impossibility of bulk compositional changes (in experiments there is no H_2O and melt loss), slow kinetics of reactions, loss of iron from silicate phases to experimental capsules, lack of equilibration, overstepping of melting reactions and difficulty of obtaining reliable glass analyses in near-solidus experiments (Ratajeski and Sisson 1999; Gardien et al. 2000; White et al. 2011; Webb et al. 2015). Nonetheless, when the low-temperature (≤720 °C) experiments are considered, with the exception of the analyses reported in Koester et al. (2002), the produced melts show low and variable Fe_{Tot}+Mg+Ti contents, overlapping the compositions of low-temperature MI (Fig. 12).

From all the above considerations, it is clear that MI are an useful tool with which to discuss the petrogenesis of granitoid rocks, and can complement experimental glasses to constrain differentiation processes occurring in anatectic magmas. Researchers working on petrogenesis of crustal granitoids can now look for and study MI in migmatites and granulites considered to be the source region of the studied magmas, or in peritectic garnet entrained in the granitoid rocks to fix the real primary composition for their specific case study. In particular, as the number of experimental studies presently reporting trace element composition of melt is limited, MI are an important contribution that provides the trace element compositions of natural anatectic melts.

Implications

Nanogranitoid melt inclusions in high-grade metamorphic rocks are a novel subject of research and are becoming a matter of considerable scientific interest, as they allow the analysis in situ of the natural primary melts produced by crustal melting. The size of nanogranitoid MI (commonly 10 μm in diameter) and of daughter minerals crystallized in them (often ≤1 μm) pose analytical challenges, and the accurate re-homogenization and compositional characterization of these small data repositories is far from being routine. However, we have shown here that, albeit slowed down by many experimental and analytical difficulties, the study of these MI opens new horizons for metamorphic and igneous petrology. Technological improvement in the coming years will make the study of MI easier, and we believe that their chemical characterization, in particular of volatiles, trace elements, and radiogenic isotopes, will provide exciting new results in many topics, such as granitoid petrogenesis, UHT and UHP metamorphism, secular variations of felsic magmatism, volatile recycling, crust formation, and silicate Earth differentiation.

Acknowledgments

Many thanks to Edward Sawyer and Chris Yakymchuck for their reviews of the manuscript and to Cal Barnes for the editorial handling. This research benefitted from funding from the Italian Ministry of Education, University, Research (Grant SIR RBSI14Y7PF to O.B. and Grant PRIN 2010TT22SC to B.C.), from Padova University (Progetti per Giovani Studiosi 2013 to O.B., Progetto di Ateneo CPDA107188/10 to B.C. and Piscopia—Marie Curie Fellowship GA No. 600376 to A.A.V.), from the Ministerio de Ciencia e Innovación of Spain (grant CGL2007-62992 to A.A.V.), and from the Alexander von Humboldt Foundation, the German Federal Ministry for Education and Research and the Deutsche Forschungsgemeinschaft (Project FE 1527/2-1 to S.F.). The research leading to these results has received funding from the European Commission, Seventh Framework Programme, under Grant Agreement no. 600376.

References cited

Acosta-Vigil, A., London, D., and Morgan, G.B. VI (2006) Experiments on the kinetics of partial melting of a leucogranite at 200 MPa H_2O and 690–800 °C: Compositional variability of melts during the onset of H_2O-saturated crustal anatexis. Contributions to Mineralogy and Petrology, 151, 539–557.

Acosta-Vigil, A., Cesare, B., London, D., and Morgan, G.B. VI (2007) Microstructures and composition of melt inclusions in a crustal anatectic environment, represented by metapelitic enclaves within El Hoyazo dacites, SE Spain. Chemical Geology, 237, 450–465.

Acosta-Vigil, A., Buick, I., Hermann, J., Cesare, B., Rubatto, D., London, D., and Morgan, G.B. VI (2010) Mechanisms of crustal anatexis: A geochemical study of partially melted metapelitic enclaves and host dacite, SE Spain. Journal of Petrology, 51, 785–821.

Acosta-Vigil, A., Buick, I., Cesare, B., London, D., and Morgan, G.B. V.I. (2012) The extent of equilibration between melt and residuum during regional anatexis and its implications for differentiation of the continental crust: A study of partially melted metapelitic enclaves. Journal of Petrology, 53, 1319–1356.

Almeev, R.R., Bolte, T., Nash, B.P., Holtz, F., Erdmann, M., and Cathey, H. (2012) High-temperature, low-H_2O silicic magmas of the Yellostone Hotspot: an experimental study of rhyolite from the Bruneau–Jarbidge eruptive center, central Snake River Plain, U.S.A. Journal of Petrology, 53, 1837–1866.

Annen, C., Blundy, J.D., and Sparks, R.S.J. (2006) The genesis of intermediate and silicic magmas in deep crustal hot zones. Journal of Petrology, 47, 505–539.

Audétat, A., and Lowenstern, J.B. (2014) Mel inclusions. In H.D. Holland and K.K. Turekian, Eds., Treatise on Geochemistry, 2nd ed., 143–173. Elsevier, Oxford.
Auzanneau, E., Vielzeuf, D., and Schmidt, M.W. (2006) Experimental evidence of decompression melting during exhumation of subducted continental crust. Contributions to Mineralogy and Petrology, 152, 125–148.
Bacon, C.R. (1989) Crystallization of accessory phases in magmas by local saturation adjacent to phenocrysts. Geochimica et Cosmochimica Acta, 53, 1055–1066.
Barbarin, B. (1988) Field evidence for successive mixing and mingling between the Piolard Diorite and the Saint-Julien-la-Vêtre Monzogranite (Nord-Forez, Massif Cen-tral, France). Canadian Journal of Earth Sciences, 25, 49–59.
——— (1999) A review of the relationships between granitoid types, their origins and their geodynamic environments. Lithos, 46, 605–626.
Barbero, L., and Villaseca, C. (1992) The Layos granite, Hercynian complex of Toledo (Spain): An example of parautochthonous restite-rich granite in a granulitic area. Transaction of the Royal Society of Edinburgh Earth Sciences, 83, 127–138.
Barich, A., Acosta-Vigil, A., Garrido, C.J., Cesare, B., Tajc□manová, L., and Bartoli, O. (2014) Microstructures and petrology of melt inclusions in the anatectic sequence of Jubrique (Betic Cordillera, S Spain): Implications for crustal anatexis. Lithos, 206–207, 303–320.
Barnes, C.G., Yoshinobu, A.S., Prestvik, T., Nordgulen, Ø., Karlsson, H., and Sundvoll, B. (2002) Mafic magma itraplating: Anatexis and hybridization in arc crust, Bindal Batholith, Norway. Journal of Petrology, 43, 2171–2190.
Bartoli, O. (2012) When the continental crust melts: A combined study of melt inclusions and classical petrology on the Ronda migmatites, 128 p. Ph.D. thesis, University of Parma, Italy.
Bartoli, O., Cesare, B., Poli, S., Bodnar, R.J., Acosta-Vigil, A., Frezzotti, M.L., and Meli, S. (2013a) Recovering the composition of melt and the fluid regime at the onset of crustal anatexis and S-type granite formation. Geology, 41, 115–118.
Bartoli, O., Tajčmanová, L., Cesare, B., and Acosta-Vigil, A. (2013b) Phase equilibria constraints on melting of stromatic migmatites from Ronda (S. Spain): Insights on the formation of peritectic garnet. Journal of Metamorphic Geology, 31, 775–789.
Bartoli, O., Cesare, B., Poli, S., Acosta-Vigil, A., Esposito, R., Turina, A., Bodnar, R.J., Angel, R.J., and Hunter, J. (2013c) Nanogranite inclusions in migmatitic garnet: Behavior during piston cylinder re-melting experiments. Geofluids, 13, 405–420.
Bartoli, O., Cesare, B., Remusat, L., Acosta-Vigil, A., and Poli, S. (2014) The H_2O content of granite embryos. Earth and Planetary Science Letters, 395, 281–290.
Bartoli, O., Acosta-Vigil, A., and Cesare, B. (2015) High-temperature metamorphism and crustal melting: working with melt inclusions. Periodico di Mineralogia, 84, http://dx.doi.org/10.2451/2015PM0434.
Becker, A., Holtz, F., and Johannes, W. (1998) Liquidus temperatures and phase compositions in the system Qz-Ab-Or at 5 kbar and very low water activities. Contributions to Mineralogy and Petrology, 130, 213–224.
Blundy, J., and Cashman, K. (2001) Ascent-driven crystallization of dacite magmas at Mount St Helens 1980–1986. Contributions to Mineralogy and Petrology, 140, 631–650.
Bodnar, R.J., and Student, J.J. (2006) Melt inclusions in plutonic rocks: Petrography and microthermometry. In J.D. Webster, Ed., Melt Inclusions in Plutonic Rocks, p. 1–26. Mineralogical Association of Canada Short Course 36.
Bowen, N.L. (1948) The granite problem and the method of multiple prejudices. In J. Gilluly, Ed., Origin of Granite, 79–90. Geological Society of America Memoir 28.
Brearley, A.J., and Rubie, D.C. (1990) Effects of H_2O on the disequilibrium breakdown of muscovite + quartz. Journal of Petrology, 31, 925–956.
Brown, M. (2013) Granite: From genesis to emplacement. Geological Society of American Bulletin, 125, 1079–1113.
Brown, M., and Rushmer, T., (2006) Evolution and Differentiation of the Continental Crust, 553 p. Cambridge University Press, U.K.
Burnham, C.W. (1967) Hydrothermal fluids at the magmatic stage. In H.L. Barnes, Ed., Geochemistry of Hydrothermal Ore Deposits, 34–76. Holt, Rinehart and Winston, New York.
——— (1975) Water and magmas: A mixing model. Geochimica et Cosmochimica Acta, 39, 1077–1084.
Candela, P.A. (1997) A review of shallow, ore-related granites: Textures, volatiles and ore metals. Journal of Petrology, 38, 1619–1633.
Carosi, R., Montomoli, C., Langone, A., Turina, A., Cesare, B., Iaccarino, S., Fascioli, L., Visonà, D., Ronchi, A., and Santa Man, R. (2015) Eocene partial melting recorded in peritectic garnets from kyanite-gneiss, Greater Himalayan Sequence, central Nepal. In S. Mukherjee, R. Carosi, P.A. van der Beek, B.K. Mukherjee, and D.M. Robinson, Eds., Tectonics of the Himalaya. Geological Society, London, Special Publications 412, pp. 111–129.
Castro, A., Patiño Douce, A.E., Corretgé, L.G., de la Rosa, J.D., El-Biad, M., and El-Hmidi, H. (1999) Origin of peraluminous granites and granodiorites, Iberian massif, Spain. An experimental test of granite petrogenesis. Contributions to Mineralogy and Petrology, 135, 255–276.
Cesare, B. (2008) Crustal melting: Working with enclaves. In E.W. Sawyer and M. Brown, Eds., Working with Migmatites, 37–55. Mineralogical Association of Canada, Short Course 38, Quebec City.
Cesare, B., and Maineri, C. (1999) Fluid-present anatexis of metapelites at El Joyazo (SE Spain): Constraints from Raman spectroscopy of graphite. Contributions to Mineralogy and Petrology, 135, 41–52.
Cesare, B., Salvioli Mariani, E., and Venturelli, G. (1997) Crustal anatexis and melt extraction during deformation in the restitic xenoliths at El Joyazo (SE Spain). Mineralogical Magazine, 61, 15–27.
Cesare, B., Marchesi, C., Hermann, J., and Gomez-Pugnaire, M.T. (2003) Primary melt inclusions in andalusite from anatectic graphitic metapelites: Implications for the position of the Al_2SiO_5 triple point. Geology, 31, 573–576.
Cesare, B., Meli, S., Nodari, L., and Russo, U. (2005) Fe^{3+} reduction during biotite melting in graphitic metapelites: another origin of CO_2 in granulites. Contributions to Mineralogy and Petrology, 149, 129–140.
Cesare, B., Maineri, C., Baron Toaldo, A., Pedron, D., and Acosta-Vigil, A. (2007) Immiscibility between carbonic fluids and granitic melts during crustal anatexis: A fluid and melt inclusion study in the enclaves of the Neogene Volcanic Province of SE Spain. Chemical Geology, 237, 433–449.
Cesare, B., Ferrero, S., Salvioli-Mariani, E., Pedron, D., and Cavallo, A. (2009) Nanogranite and glassy inclusions: the anatectic melt in migmatites and granulites. Geology, 37, 627–630.
Cesare, B., Acosta-Vigil, A., Ferrero, S., and Bartoli, O. (2011) Melt inclusions in migmatites and granulites. In M.A. Forster and J.D. Fitz Gerald, Eds., The Science of Microstructure—Part II, paper 2. Journal of the Virtual Explorer, Electronic Edition 38.
Cesare, B., Acosta-Vigil, A., Bartoli, O., and Ferrero, S. (2015) What can we learn from melt inclusions in migmatites and granulites? Lithos, 239, 186–216.
Chappell, B.W. (1984) Source rocks of I- and S-type granites in the Lachlan Fold Belt, southeastern Australia. Philosophical Transactions of the Royal Society of London A, 310, 693–707.
——— (1999) Aluminium saturation in I- and S-type granites and the characterization of fractionated haplogranites. Lithos, 46, 535–551.
Chappell, B.W., and White, A.J.R. (1974) Two contrasting granite types. Pacific Geology, 8, 173–174.
——— (1992) I- and S-type granites in the Lachlan Fold Belt. Transactions of the Royal Society of Edinburgh Earth Sciences, 83, 1–26.
——— (2001) Two contrasting granite types: 25 years later. Australian Journal of Earth Sciences, 48, 489–499.
Chappell, B.W., White, A.J.R., and Wyborn, D. (1987) The importance of residual source material (restite) in granite petrogenesis. Journal of Petrology, 28, 1111–1138.
Clemens, J.D. (2003) S-type granitic magmas—petrogenetic issues, models and evidence. Earth Science Reviews, 61, 1–18.
——— (2006) Melting of the continental crust: Fluid regimes, melting reactions and source-rock fertility. In M. Brown, and T. Rushmer, Eds., Evolution and Differentiation of the Continental Crust, p. 297–331. Cambridge University Press, U.K.
Clemens, J.D., and Mawer, C.K. (1992) Granitic magma transport by fracture propagation. Tectonophysics, 204, 339–360.
Clemens, J.D., and Stevens, G. (2012) What controls chemical variation in granitic magmas? Lithos, 134-135, 317–329.
——— (2015) Comment on "Water-fluxed melting of the continental crust: A review" by R.F. Weinbert and P. Hasalová. Lithos, 234-235, 100–101.
Clemens, J.D., and Watkins, J.M. (2001) The fluid regime of high-temperature metamorphism during granitoid magma genesis. Contributions to Mineralogy and Petrology, 140, 600–606.
Clocchiatti, R. (1975) Les inclusions vitreuses des cristaux de quartz. Étude optique, thermooptique et chimique. Applications géologiques, Mémoires de la Société géologique de France, 122, 1–96.
Conrad, W.K., Nicholls, I.A., and Wall, V.J. (1988) Water-saturated and -undersaturated melting of metaluminous and peraluminous crustal compositions at 10 kbar: Evidence for the origin of silicic magmas in the Taupo volcanic zone, New Zealand, and other occurrences. Journal of Petrology, 29, 765–803.
Darling, R.S. (2013) Zircon-bearing, crystallized melt inclusions in peritectic garnet from the western Adirondack Mounatins, New York State, U.S.A. Geofluids, 13, 453–459.
DePaolo, D.J. (1981) Trace element and isotopic effects of combined wallrock assimilation and fractional crystallization. Earth and Planetary Science Letters, 53, 189–202.
Droop, G.T.R., Clemens, J.D., and Dalrymple, J. (2003) Processes and conditions during contact anatexis, melts escape and restite formation: The Huntly Gabbro complex, NE Scotland. Journal of Petrology, 44, 995–1029.
Ebadi, A., and Johannes, W. (1991) Beginning of melting and composition of first melts in the system Qz-Ab-Or-H_2O-CO_2. Contributions to Mineralogy and Petrology, 106, 286–295.
Esposito, E., Klebesz, R., Bartoli, O., Klyukin, Y.I., Moncada, D., Doherty, A., and Bodnar, R.J. (2012) Application of the Linkam TS1400XY heating stage to melt inclusion studies. Central European Journal of Geosciences, 4/2, 208–218.
Farina, F., Albert, C., and Lana, C. (2015) The Neoarchean transition between medium- and high-K granitoids: Clues from the Southern São Francisco Craton (Brazil). Precambrian Research, 266, 375–394.
Faure, F., and Schiano, P. (2005) Experimental investigation of equilibration conditions during forsterite growth and melt inclusion formation. Earth and Planetary Science Letters, 236, 882–898.
Ferrero, S., Bodnar, R.J., Cesare, B., and Viti, C. (2011) Reequilibration of primary fluid inclusions in peritectic garnet from metapelitic enclaves, El Hoyazo, Spain. Lithos, 124, 117–131.
Ferrero, S., Bartoli, O., Cesare, B., Salvioli-Mariani, E., Acosta-Vigil, A., Cavallo, A., Groppo, C., and Battiston, S. (2012) Microstructures of melt inclusions in

anatectic metasedimentary rocks. Journal of Metamorphic Geology, 30, 303–322.
Ferrero, S., Braga, R., Berkesi, M., Cesare, B., and Laridhi Ouazaa, N. (2014) Production of metaluminous melt during fluid-present anatexis: An example from the Maghrebian basement, La Galite Archipelago, central Mediterranean. Journal of Metamorphic Geology, 32, 209–225.
Ferrero, S., Wunder, B., Walczak, K., O'Brien, P.J., and Ziemann, M.A. (2015) Preserved near ultrahigh-pressure melt from continental crust subducted to mantle depths. Geology, 43, 447–450.
Ferrero, S., Ziemann, M.A., Angel, R.J., O'Brien, P.J., and Wunder, B. (2016) Kumdykolite, kokchetavite and cristobalite crystallized in nanogranites from felsic granulites, Orlica-Snieznik Dome (Bohemian Massif): Not an evidence for ultrahigh-pressure conditions. Contributions to Mineralogy and Petrology, 171, DOI: 10.1007/s00410-015-1220-x.
Ferri, F., Poli, S., and Vielzeuf, D. (2009) An experimental determination of the effect of bulk composition on phase relationships in metasediments at near-solidus conditions. Journal of Petrology, 50, 909–993.
Frezzotti, M.L. (2001) Silicate melt inclusions in magmatic rocks: Applications to petrology. Lithos, 55, 273–299.
Frost, B.R., and Frost, C.D. (2008) A geochemical classification for feldspathic igneous rocks. Journal of Petrology, 49, 1955–1969.
Frost, B.R., Barnes, C.G., Collins, W.J., Arculus, R.J., Ellis, D.J., and Frost, C.D. (2001) A geochemical classification for granitic rocks. Journal of Petrology, 42, 2033–2048.
Gaetani, G.A., O'Leary, J.A., Shimizu, N., Bucholz, C.E., and Newville, M. (2012) Rapid reequilibration of H_2O and oxygen fugacity in olivine-hosted melt inclusions. Geology, 40, 915–918.
García-Casco, A., Haissen, F., Castro, A., El-Hmidi, H., Torres-Roldán, R.L., and Millán, G. (2003) Synthesis of staurolite in melting experiments of a natural metapelite: Consequences for phase relations in low-temperature pelitic migmatites. Journal of Petrology, 44, 1727–1757.
Gardien, V., Thompson, A.B., Grujic, D., and Ulmer, P. (1995) Experimental melting of biotite + plagioclase + quartz ± muscovite assemblages and implications for crustal melting. Journal of Geophysical Research, 100, 15581–15591.
Gardien, V., Thompson, A.B., and Ulmer, P. (2000) Melting of biotite + plagioclase + quartz gneisses: The role of H_2O in the stability of amphibole. Journal of Petrology, 41, 651–666.
Gualda, G.A., and Ghiorso, M.S. (2013) The Bishop Tuff magma body: An alternative to the Standard Model. Contributions to Mineralogy and Petorlogy, 166, 755–775.
Gilluly, J. (1948) Origin of Granite, 139 p. Geological Society of America Memoir 28.
Grant, J.A. (2004) Liquid compositions from low-pressure experimental melting of pelitic rock from Morton Pass, Wyoming, U.S.A. Journal of Metamorphic Geology, 22, 65–78.
——— (2009) THERMOCALC and experimental modeling of melting of pelite, Morton Pass, Wyoming. Journal of Metamorphic Geology, 27, 571–578.
Gray, C.M., and Kemp, A.I.S. (2009) The two-component model for the genesis of granitic rocks in southeastern Australia—Nature of the metasedimentary-derived and basaltic end members. Lithos, 111, 113–124.
Groppo, C., Rolfo, F., and Indares, A. (2012) Partial melting in the Higher Himalaya Crystallines of eastern Nepal: The effect of decompression and implications for the "Channel Flow" model. Journal of Petrology, 53, 1057–1088.
Guernina, S., and Sawyer, E.W. (2003) Large-scale melt-depletion in granulite terranes: An example from the Archean Ashuanipi subprovince of Quebec. Journal of Metamorphic Geology, 21, 181–201.
Guillot, S., and Le Fort, P. (1995) Geochemical constraints on the bimodal origin of High Himalayan leucogranites. Lithos, 35, 221–234.
Hacker, R., Kelemen, P.B., and Behn, M.D. (2011) Differentiation of the continental crust by relamination. Earth and Planetary Science Letters, 307, 501–516.
Halter, W.E., Pettke, T., Heinrich, C.A., and Rothen-Rutishauser, B. (2002) Major to trace element analysis of melt inclusions by laser-ablation ICP–MS: Methods of quantification. Chemical Geology, 183, 63–86.
Harris, N., and Massey, J. (1994) Decompression and anatexis of Himalayan metapelites. Tectonics, 13, 1537–1546.
Harris, N.B.W., Vance, D., and Ayers, M. (2000) From sediment to granite: Time scales of anatexis in the upper crust. Chemical Geology, 162, 155–167.
Hauri, E. (2002) SIMS analysis of volatiles in silicate glasses, 2: Isotopes and abundances in Hawaiian melt inclusions. Chemical Geology, 183, 115–141.
Hermann, J., and Spandler, C. (2008) Sediment melts at sub-arc depths: An experimental study. Journal of Petrology, 49, 717–740.
Holtz, F., and Johannes, W. (1991) Genesis of peraluminous granites: I. Experimental investigation of melt compositions at 3 and 5 kb and various H_2O activities. Journal of Petrology, 32, 935–958.
Holtz, F., Johannes, W., and Pichavant, M. (1992) Effect of excess aluminium on phase relations in the system Qz-Ab-Or: Experimental investigation at 2 kbar and reduced H_2O-activity. European Journal of Mineralogy, 4, 137–152.
Huang, W.L., and Wyllie, P.J. (1975) Melting reactions in the system $NaA1Si_3O_8$-$KA1Si_3O_8$-SiO_2 to 35 kilobars, dry and with excess water. Journal of Geology, 83, 737–748.
——— (1981) Phase relationships of S-type granite with H_2O to 35 kbar: Muscovite granite from Harney Peak, South Dakota. Journal of Geophysical Research, 86, 10515–10529.
Huizenga, J.M., and Touret, J.L.R. (2012) Granulites, CO_2 and graphite. Gondwana Research, 22, 799–809.
Iaccarino, S., Montomoli, C., Carosi, R., Massonne, H.-J., Langone, A., and Visonà, D. (2015) Pressure-temperature-time-deformation path of kyanite-bearing migmatitic paragneiss in the Kali Gandaki valley (Central Nepal): Investigation of Late Eocene–Early Oligocene melting processes. Lithos, 231, 103–121.
Icenhower, J., and London, D. (1995) An experimental study of element partitioning among biotite, muscovite and coexisting peraluminous silicic melt at 200 MPa (H_2O). American Mineralogist, 80, 1229–1251.
——— (1996) Experimental partitioning of Rb, Cs, Sr, and Ba between alkali feldspar and peraluminous melt. American Mineralogist, 81, 719–734.
Jamieson, R.A., Unsworth, M.J., Harris, N.G.W., Rosenberg, C., and Schulmann, K. (2011) Crustal melting and the flow of mountains. Elements, 7, 253–260.
Johannes, W., and Holtz, F. (1996) Petrogenesis and Experimental Petrology of Granitic Rocks, 335 p. Berlin, Springer.
Kawakami, T., Yamaguchi, I., Miyake, A., Shibata, T., Maki, K., Yokoyama, T.D., and Hirata, T. (2013) Behavior of zircon in the upper-amphibolite to granulite facies schist/migmatite transition, Ryoke metamorphic belt, SW Japan: Constraints from the melt inclusions in zircon. Contributions to Mineralogy and Petrology, 165, 575–591.
Kemp, A.I.S., Hawkesworth, C.J., Foster, G.L., Paterson, B.A., Woodhead, J.D., Hergt, J.M., Gray, C.M., and Whitehouse, M.J. (2007) Magmatic and crustal differentiation history of granitic rocks from Hf-O isotopes in zircon. Science, 315, 980–983.
Kent, A.J.R. (2008) Melt inclusions in basaltic and related volcanic rocks. Reviews in Mineralogy and Geochemistry, 69, 273–331.
Kesler, S.E., Bodnar, R.J., and Mernagh, T.P. (2013) Role of fluid and melt inclusion studies in geologic research. Geofluids, 13, 398–404.
Koester, E., Pawley, A.R., Fernandes, L.A.D., Porcher, C.C., and Soliani, E. Jr. (2002) Experimental melting of cordierite gneiss and the petrogenesis of syntranscurrent peraluminous granites in southern Brazil. Journal of Petrology, 43, 1595–1616.
Korhonen, F.J., Saito, S., Brown, M., and Siddoway, C.S. (2010) Modeling multiple melt loss events in the evolution of an active continental margin. Lithos, 116, 230–248.
Kretz, R. (1983) Symbols for rock-forming minerals. American Mineralogist, 68, 277–279.
Le Breton, N., and Thompson, A.B. (1988) Fluid-absent (dehydration) melting of biotite in metapelites in the early stages of crustal anatexis. Contributions to Mineralogy and Petrology, 99, 226–237.
Le Fort, P. (1981) Manaslu leucogranite: A collision signature of the Himalaya. A model for its genesis and emplacement. Journal of Geophysical Research, 86, 10545–10568.
Le Fort, P., Cuney, M., Deniel, C., France-Lanord, C., Sheppard, S.M.F., Upreti, B.N., and Vidal, P. (1987) Crustal generation of the Himalayan leucogranites. Tectonophysics, 134, 39–57.
Lesher, C.E., Walker, D., Candela, P., and Hays, J.F. (1982) Soret fractionation of natural silicate melts of intermediate to silicic composition. Geological Society of America Abstracts with Programs, 14, 545.
Litvinovsky, B.A., Steele, I.M., and Wickham, S.M. (2000) Silicic magma formation in overthickened crust: Melting of charnockite and leucogranite at 15, 20 and 25 kbar. Journal of Petrology, 41, 717–737.
López, S., Castro, A., and García-Casco, A. (2005) Production of granodiorite melt by interaction between hydrous mafic magma and tonalitic crust. Experimental constraints and implications for the generation of Archaean TTG complexes. Lithos, 79, 229–250.
Luth, W.C., Jahns, R.H., and Tuttle, O.F. (1964) The granite system at pressure of 4 to 10 kilobars. Journal of Geophysical Research, 69, 759–773.
Maheshwari, A., Coltorti, M., Sial, A.N., and Mariano, G. (1996) Crustal influences in the petrogenesis of the Malani rhyolite, southwestern Rajasthan: Combined trace element and oxygen isotope constraints. Journal of the Geological Society of India, 47, 611–619.
Massare, D., Metrichm, N., and Clocchiatti, R. (2002) High-temperature experiments on silicate melt inclusions in olivine at 1 atm: Inference on temperatures of homogenization and H_2O concentrations. Chemical Geology, 183, 87–98.
Massonne, H.J. (2014) Wealth of *P*-*T*-t information in medium-high grade metapelites: Example from the Jubrique Unit of the Betic Cordillera, S Spain. Lithos, 208-209, 137–157.
Miller, C.F., McDowell, S.M., and Mapes, R.W. (2003) Hot and cold granites? Implications of zircon saturation temperatures and preservation of inheritance. Geology, 31, 529–532.
Milord, I., Sawyer, E.W., and Brown, M. (2001) Formation of diatexite migmatite and granite magma during anatexis of semipelitic metasedimentary rocks: An example from St. Malo, France. Journal of Petrology, 42, 487–505.
Montel, J.M. (1993) A model for monazite/melt equilibrium and applications to the generation of granitic magmas. Chemical Geology, 110, 127–146.
Montel, J.M., and Vielzeuf, D. (1997) Partial melting of metagraywackes. Part II. Compositions of minerals and melts. Contributions to Mineralogy and Petrology, 128, 176–196.
Morgan, G.B. VI, and London, D. (1996) Optimizing the electron microprobe analysis of hydrous alkali aluminosilicate glasses. American Mineralogist, 81, 1176–1185.
——— (2005a) Effect of current density on the electron microprobe analysis of alkali aluminosilicate glasses. American Mineralogist, 90, 1131–1138.

——— (2005b) Phosphorus distribution between potassic alkali feldspar and metaluminous haplogranitic liquid at 200 MPa (H_2O): The effect of undercooling on crystal-liquid systematics. Contributions to Mineralogy and Petorlogy, 150, 456–471.
Mosca, P., Groppo, C., and Rolfo, F. (2012) Structural and metamorphic features of the Main Central Trust Zone and its contiguous domains in the eastern Nepalese Himalaya. Journal of Virtual Explorer, paper 2, Electronic Edition 41.
Nair, R., and Chacko, T. (2002) Fluid-absent melting of high-grade semi-pelites: *P*–*T* constraints on orthopyroxene formation and implications for granulite genesis. Journal of Petrology, 43, 2121–2141.
O'Connor, J.T. (1965) A classification for quartz-rich igneous rocks based on feldspar ratios. U.S. Geological Survey Professional Paper, 525, 79–84.
Olsen, S.N., and Grant, J.A. (1991) Isocon analysis of migmatization in the Front Range, Colorado U.S.A. Journal of Metamorphic Geology, 9, 151–164.
Pandit, M.K., Shekhawat, L.S., Ferreira, V.P., Sial, A.N., and Bohra, S.K. (1999) Trondhjemite and granodiorite assemblages from west of Barmer: Probable basement for malani Magmatism in western India. Journal Geological Society of India, 53, 89–96.
Patiño Douce, A.E., and Beard, J.S. (1995) Dehydration-melting of biotite gneiss and quartz amphibolite from 3 to 15 kbar. Journal of Petrology, 36, 707–738.
——— (1996) Effects of *P*, $f(O_2)$ and Mg/Fe ratio on dehydration-melting of model metagraywackes. Journal of Petrology, 37, 999–1024.
Patiño Douce, A.E., and Harris, N. (1998) Experimental constraints on Himalayan anatexis. Journal of Petrology, 39, 689–710.
Patiño Douce, A.E., and Johnston, A.D. (1991) Phase equilibria and melt productivity in the pelitic system: Implications for the origin of peraluminous granitoids and aluminous granulites. Contributions to Mineralogy and Petrology, 107, 202–218.
Peto, P. (1976) An experimental investigation of melting relationships involving muscovite and paragonite in the silica-saturated portion of the system K_2O-Na_2O-Al_2O_3-SiO_2-H_2O to 15 kbar total pressure. In Progress in Experimental Petrology, 3rd Report, p. 41–45. NERC, London.
Pickering, J.M., and Johnston, D.A. (1998) Fluid-absent melting behaviour of a two mica metapelite: Experimental constraints on the origin of Black Hill Granite. Journal of Petrology, 39, 1787–1804.
Portnyagin, M., Almeev, R., Matveev, S., and Holtz, F. (2008) Experimental evidence for rapid H_2O exchange between melt inclusions in olivine and host magma. Earth and Planetary Science Letters, 272, 541–552.
Ratajeski, K., and Sisson, T.W. (1999) Loss of iron to gold capsules in rock-melting experiments. American Mineralogist, 84, 1521–1527.
Read, H.H. (1948) Granites and granites. In J. Gilluly, Ed., Origin of Granite, p. 1–19. Geological Society of America Memoir 28.
Roedder, E. (1979) Origin and significance of magmatic inclusions. Bulletin of Mineralogy, 102, 487–510.
——— (1984) Fluid Inclusions, vol. 12. Reviews in Mineralogy, Mineralogical Society of America, Chantilly, Virginia.
Rosenberg, C.L., and Handy, M.R. (2005) Experimental deformation of partially melted granite revisited: implications for the continental crust. Journal of Metamorphic Geology, 23, 19–28.
Rudnick, R.L., and Gao, S. (2014) Composition of the Continental Crust. In R.L. Rudnick Ed., Treatise on Geochemistry, 2nd ed., 1–51.
Sawyer, E.W. (2008) Atlas of migmatites. Mineralogical Association of Canada, The Canadian Mineralogist Special Publication 9, Quebec City.
Sawyer, E.W., Cesare, B., and Brown, M. (2011) When the continental crust melts. Elements, 7, 229–234.
Santosh, M., and Omori, S. (2008) CO_2 flushing: a plate tectonic perspective. Gondwana Research, 13, 86–102.
Scaillet, B., France-Lanord, C., and Le Fort, P. (1990) Badrinath-Gangotri plutons (Garhwal, India): Petrological and geochemical evidence for fractionation processes in a high Himalayan leucogranite. Journal of Volcanology and Geothermal Research, 44, 163–188.
Scaillet, B., Pichavant, M., and Roux, J. (1995) Experimental crystallization of leucogranite magmas. Journal of Petrology, 36, 664–706.
Schiano, P. (2003) Primitive mantle magmas recorded as silicate melt inclusions in igneous minerals. Earth Science Reviews, 63, 121–144.
Schmidt, M.W., Vielzeuf, D., and Auzanneau, E. (2004) Melting and dissolution of subducting crust at high pressures: The key role of white mica. Earth and Planetary Science Letters, 228, 65–84.
Sharma, K.K. (2004) The Neoproterozoic Malani magmatism of the northwestern India shield: Implications for crust-building processes. Proceedings of the Indian Academy of Science, 113, 795–807.
Singh, J., and Johannes, W. (1996) Dehydration melting of tonalities. Part II. Composition of melts and solids. Contributions to Mineralogy and Petrology, 125, 26–44.
Skjerlie, K.P., and Johnston, A.D. (1993) Fluid-absent melting behavior of an F-rich tonalitic gneiss at med-crustal pressures: Implications for the generation of anorogenic granites. Journal of Petrology, 34, 785–815.
Slagstad, T., Jamieson, R.A., and Culshaw, N.G. (2005) Formation, crystallization, and migration of melt in the mid-orogenic crust: Muskoka domain migmatites, Grenville Province, Ontario. Journal of Petrology, 46, 893–919.
Sobolev, A.V. (1996) Melt inclusions in minerals as a source of principle petrological information. Petrology, 4, 209–220.
Solar, G.S., and Brown, M. (2001) Petrogenesis of migmatites in Maine, U.S.A.: Possible source of peraluminous leucogranite in plutons. Journal of Petrology, 42, 789–823.
Sorby, H.C. (1858) On the microscopical structure of crystals, indicating origin of minerals and rocks. Quarterly Journal of the Geological Society of London 14, 453–500.
Spicer, E.M., Stevens, G., and Buick, I.S. (2004) The low-pressure partial-melting behaviour of natural boron-bearing metapelites from the Mt. Stafford area, central Australia. Contributions to Mineralogy and Petrology, 148, 160–179.
Stevens, G., Villaros, A., and Moyen, J.-F. (2007) Selective peritectic garnet entrainment as the origin of geochemical diversity in S-type granites. Geology, 35, 9–12.
Sun, S.S., and McDonough, W.F. (1989) Chemical and isotopic systematics of oceanic basalts: Implications for mantle composition and processes. In A.D. Saunders and M.J. Norry, Eds., Magmatism in the Ocean Basins, p. 313–345. Geological Society, London, Special Publications 42.
Symmes, G.H., and Ferry, J.M. (1995) Metamorphism, fluid-flow and partial melting in pelitic rocks from the Onawa contact aureole, central Maine, U.S.A. Journal of Petrology, 36, 587–612.
Thomas, R., and Davidson, P. (2012) H_2O in granite and pegmatite-forming melts. Ore Geology Reviews, 46, 32–46.
Thompson, A.B. (1990) Heat, fluids, and melting in the granulite facies. In D. Vielzeuf and P. Vidal, Eds., Granulites and Crustal Evolution, p. 37–57. NATO ASI Series vol. 311.
Tropper, P., Konzett, J., and Finger, F. (2005) Experimental constraints on the formation of high-*P*/high-*T* granulites in the Southern Bohemian Massif. European Journal of Mineralogy, 17, 343–356.
Tuttle, O.F., and Bowen, N.L. (1958) Origin of granite in the light of experimental studies in the system: $NaAlSi_3O_8$-$KAlSi_3O_8$-SiO_2-H_2O. Geological Society of America Memoir, 74, 153 p.
Vernon, R.H. (2010) Granites really are magmatic: Using microstructural evidence to refute some obstinate hypotheses. In M.A. Forster and J.D. Fitz Gerald, Eds., The Science of Microstructure—Part I, paper 1. Journal of the Virtual Explorer, Electronic Edition 35.
Vielzeuf, D., and Holloway, J.R. (1988) Experimental determination of the fluid-absent melting relations in the pelitic system. Contributions to Mineralogy and Petrology, 98, 257–276.
Villaros, A., Stevens, G., Moyen, J.F., and Buick, I.S. (2009) The trace element compositions of S-type granites: Evidence for disequilibrium melting and accessory phase entrainment in the source. Contributions to Mineralogy and Petrology, 158, 543–561.
Visonà, D., Carosi, R., Montomoli, C., Peruzzo, L., and Tiepolo, M. (2012) Miocene andalusite leucogranite in central-east Himalaya (Everest-Masang Kang area): Low-pressure melting during heating. Lithos, 144, 194–208.
Wall, V.J., Clemens, J.D., and Clarke, D.B. (1987) Models for granitoid evolution and source compositions. Journal of Geology, 95, 731–750.
Ward, R., Stevens, G., and Kisters, A. (2008) Fluid and deformation induced partial melting and melt volumes in low-temperature granulite-facies metasediments, Damara Belt, Namibia. Lithos, 105, 253–271.
Watkins, J.M., Clemens, J.D., and Treloar, P.J. (2007) Archaean TTGs as sources of younger granitic magmas: melting of sodic metatonalites at 0.6–1.2 GPa. Contributions to Mineralogy and Petrology, 154, 91–110.
Watson, E.B., and Harrison, T.M. (1984) Accessory minerals and the geochemical evolution of crustal magmatic systems: A summary and prospectus of experimental approaches. Physics of the Earth and Planetary Interiors, 35, 19–30.
Webb, G., Powell, R., and McLaren, S. (2015) Phase equilibria constraints on the melt fertility of crustal rocks: The effect of subsolidus water loss. Journal of Metamorphic Geology, 33, 147–165.
Weinberg, R.F., and Hasalovà, P. (2015a) Water-fluxed melting of the continental crust: A review. Lithos, 212-215, 158–188.
——— (2015b) Reply to comment by J.D. Clemens and G. Stevens on "Water-fluxed melting of the continental crust: A review." Lithos, 234-235, 102–103.
Weinberg, R.F., Sial, A.N., and Pessoa, R.R. (2001) Magma flow within the Tavares pluton, northeastern Brazil: Compositional and thermal convection. Geological Society of America Bulletin, 113, 508–520.
White, R.W., Stevens, G., and Johnson, T.E. (2011) Is the crucible reproducible? Reconciling melting experiments with thermodynamic calculations. Elements, 7, 241–246.
Wilke, S., Klahn, C., Bolte, T., Almeev, R., and Holtz, F. (2015) Experimental investigation of the effect of Ca, Fe and Ti on cotectic compositions of the rhyolitic system. European Journal of Mineralogy, DOI: 10.1127/ejm/2015/0027-2423.
Yakymchuk, C., Brown, C.B., Brown, M., Siddoway, C., Fanning, C.M., and Korhonen, F.J. (2015) Paleozoic evolution of western Marie Byrd Land, Antarctica. Geological Society of American Bulletin, 127, 1464–1484.
Zeck, H.P. (1970) An erupted migmatite from Cerro de Hoyazo, SE Spain. Contributions to Mineralogy and Petrology, 26, 225–246.

Manuscript received August 24, 2015
Manuscript accepted January 22, 2016
Manuscript handled by Calvin Barnes